

Electron transfer reactions within σ - and π -bridged dinitrogen-centered intervalence radical cations

STEPHEN F. NELSEN

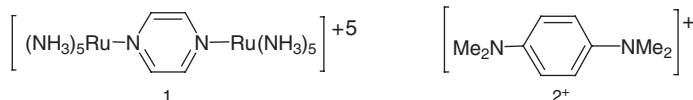
Department of Chemistry, University of Wisconsin, Madison, WI 53716 1396, USA

| | | |
|---|--|-----|
| 1 | Introduction | 183 |
| 2 | Determination of k_{ESR} values for σ -bridged systems | 187 |
| 3 | Determination of k_{ET} values for π -bridged systems | 192 |
| 4 | Determination of ET parameters from the IV band | 196 |
| | IV Bandwidth | 196 |
| | Estimation of the ET distance | 197 |
| 5 | Ion-pairing effects | 198 |
| 6 | Separation of λ_s from λ_v | 200 |
| 7 | Calculation of k_{opt} from optical data using adiabatic theory | 204 |
| 8 | BJ treatment for ET within IV compounds | 208 |
| 9 | Effects of low-bridge-oxidized excitation energies | 211 |
| | Acknowledgements | 212 |
| | References | 212 |

1 Introduction

We will discuss intramolecular electron transfer (ET) between the charge-bearing units (**M** groups) of symmetrical intervalence (IV) compounds in this chapter. IV compounds are a concept introduced by inorganic chemists, and were reviewed at length by Robin and Day¹ and by Allen and Hush² in 1967. IV compounds refer to specific oxidation levels of compounds having two (or more) **M** groups, originally metals and their attached ligands, which are joined by a bidentate ligand called the bridge (**B**). If the charges on the **M** groups are integers and the same at one oxidation level, addition or removal of an electron produces an IV oxidation level, which might have different charges on the **M** groups. Robin and Day assigned three classes of IV compounds that are still in use.¹ Class I refers to compounds that have no electronic interaction between the **M** groups through the bridge, and are of little interest here. Class II refers to compounds that have a small enough electronic interaction that charge is nearly localized on one **M** group. They may be usefully thought of as $\mathbf{M}^+ - \mathbf{B} - \mathbf{M}^0$ (if the overall charge is +1). Class III compounds have such a large interaction that they are delocalized, with the same fractional charge on the **M** groups, $\mathbf{M}^{1/2} - \mathbf{B} - \mathbf{M}^{1/2}$ (if the overall charge is +1). The first designed IV compound was the Creutz-Taube complex, **1**, published in 1969.³ People are still

discussing whether **1** is Class II or III, and



Meyer and coworkers have assigned it and related compounds to a special intermediate class, “II/III”.⁴ Despite the fact that the first organic radical cations ever isolated were *p*-phenylene diamine derivatives including **2**⁺, organic chemists did not devise the *IV* compound concept; **2** is obviously very closely related structurally to **1**: the charge-bearing unit is a dimethylamino unit, and bonding to the bridge is with N–C covalent bonds instead of Ru–N coordination bonds. Apparently no organic chemist ever thought that **2**⁺ had a chance of being anything but a delocalized compound with equal partial positive charges at N. Apparently the first mention of an all-organic *IV* compound was by Cowan and coworkers in a review of ferrocene chemistry, who pointed out that tetrathiofulvalene radical cation was a Class III *IV* compound in 1973.⁵

Class II *IV* compounds are the simplest ET systems known, because the bridge holds the **M** groups in specific orientations relative to each other (so there might actually be a single orientation associated with a single electronic coupling involved in the ET), and the driving force for the ET reaction is zero. Hush pointed out early that Class II compounds have especially revealing optical spectra.⁶ They show an unusually broad nearly Gaussian-shaped absorption band, and using the two-state model having parabolic diabatic surfaces that was employed by Marcus (see Fig. 1),^{7,8} the transition energy at the band maximum ($\bar{\nu}_{\text{max}}$, often called E_{op}) is equal to Marcus’s λ , the vertical reorganization energy on the diabatic surfaces, which is the energy difference between the minimum of one parabola and the other one. The

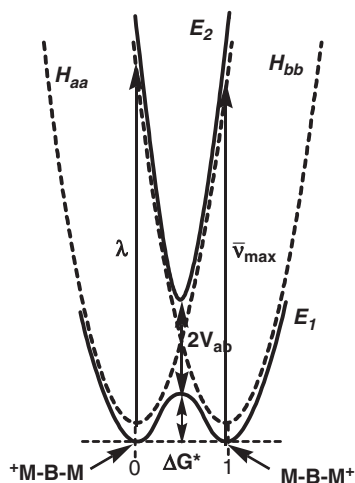


Fig. 1 Marcus–Hush classical two-state model for a Class II *IV* compound.

diabatic surfaces in Fig. 1 are shown as the dotted parabolas, which would be the energy surfaces for a Class I compound. Class II compounds have modest electronic interaction between the **M** groups through the bridge, leading to the energy separation at the transition state for ET of $2V_{ab}$, using the classical two-state Hamiltonian equation to describe the system:

$$\begin{vmatrix} H_{aa} - E & V_{ab} \\ V_{ab} & H_{bb} - E \end{vmatrix} = 0 \quad (1)$$

Both Hush and Marcus emphasized that the justification for Equation (1) is perturbation theory, so that V_{ab} should be small (relative to λ), but Newton and coworkers have noted that the solutions to Equation (1)⁸ are mathematically valid for any V_{ab} .⁹ Sutin explicitly gave the equations for E_1 and E_2 that are obtained from Equation (1) using parabolic diabatic surfaces:⁸

$$E_1 = 0.5[\lambda(2X^2 - 2X + 1) + \Delta G^\circ] - 0.5\{[\lambda(2X - 1) - \Delta G^\circ]^2 + 4(H_{AB})^2\}^{1/2}$$

$$E_2 = 0.5[\lambda(2X^2 - 2X + 1) + \Delta G^\circ] + 0.5\{[\lambda(2X - 1) - \Delta G^\circ]^2 + 4(H_{AB})^2\}^{1/2} \quad (2)$$

which produce the energy surfaces shown in Fig. 2 and Table 1 for $\lambda = 14,000 \text{ cm}^{-1}$ (which is about its size for the 5-bond-bridged Hy_2Ar^+ compounds discussed below). This two-state model refers to what is called the superexchange mechanism for ET, where the charge never becomes localized on the bridge, so the species having a symmetrical charge distribution is an energy maximum.^{8,10}

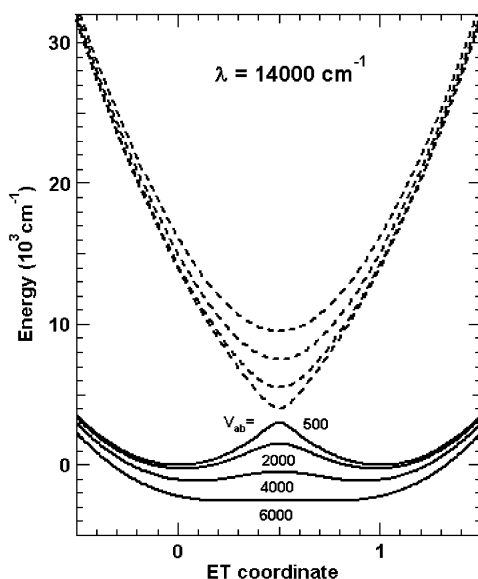


Fig. 2 Classical Marcus-Hush energy surfaces showing the decrease in barrier for $\lambda = 14,000$, $V_{ab} = 500\text{--}6000 \text{ cm}^{-1}$. Both the upper surfaces (dashed lines) and the lower ones (solid lines) are shown.

Table 1 Classical two-state adiabatic surfaces at $\lambda = 14,000 \text{ cm}^{-1}$

| V_{ab} | H_{ab}/λ | $E_{1\min}$ | X_{\min} | ΔG^* | F |
|----------|------------------|-------------|------------|--------------|------|
| 500 | 0.04 | -17.9 | 0.001 | 3018 | 0.86 |
| 1000 | 0.07 | -71.4 | 0.005 | 2571 | 0.73 |
| 2000 | 0.14 | -286 | 0.021 | 1786 | 0.51 |
| 4000 | 0.29 | -1143 | 0.090 | 643 | 0.18 |
| 6000 | 0.43 | -2571 | 0.242 | 71 | 0.02 |

The ET transition state is the ground state (E_1) maximum, which occurs at energy $\lambda/4 - V_{ab}$, and at $X = 0.5$ for all V_{ab} . As V_{ab} increases, the adiabatic energy minima (closest one to zero at $X_{\min} = 1/2\{1 - [1 - 4(V_{ab}^2/\lambda^2)]^{1/2}\}$) are stabilized relative to the diabatic minima by V_{ab}^2/λ and they pinch in towards the transition state on the X -axis. X_{\min} corresponds to the square of Mulliken's linear charge transfer combination coefficient, c ,¹¹ which is the same as Hush's mixing coefficient, α .⁶

The ET barrier on the adiabatic surface, ΔG^* (Fig. 1), is given by:

$$\Delta G^* = \lambda/4 - V_{ab} + V_{ab}^2/\lambda \quad (3)$$

In early articles, various authors have used only its first or first two terms, which are reasonable approximations if V_{ab}/λ is small enough. At X_{\min} the separation of the adiabatic surfaces is λ , the same as the separation of the diabatic surfaces at their minimum. The separation of the diabatic surfaces at X_{\min} is $\lambda[1 - 4V_{ab}^2/\lambda^2]^{1/2}$.¹² The fraction F of the $\lambda/4$ barrier on the diabatic surfaces that remains as V_{ab} increases is $F = [1 - 2(V_{ab}/\lambda)]^2$.¹³ ΔG^* becomes 0 and the charge becomes delocalized when V_{ab} increases to $\lambda/2$ [where $E_1(X = 0.5) = -\lambda/4$]. At higher values of V_{ab} , there is only a single minimum for E_1 at $X = 0.5$.

Obtaining λ for an IV compound using Equation (1) is trivial, it is simply the IV band transition energy. Hush introduced evaluating V_{ab} and hence the ET barrier from the IV band of optical spectrum using the following equation:⁶

$$V_{ab} = (|\mu_{12}|/|\Delta\mu_{ab}|)\bar{v}_{\max} = (|\mu_{12}|/|ed_{ab}|)\bar{v}_{\max} \quad (4)$$

where μ_{12} is the transition dipole moment (an experimental quantity, so it occurs on the adiabatic surfaces that the molecule actually occupies) and $\Delta\mu_{ab}$ is the change in dipole moment (on the theoretical, diabatic surfaces), which is approximated as the electron charge times d_{ab} , the ET distance on the diabatic surfaces. This number was taken to be the metal-metal distance. Hush also introduced the familiar Gaussian approximation:

$$V_{ab} = 2.06 \times 10^{-2} (\epsilon_{\max} \Delta\bar{v}_{1/2} \bar{v}_{\max})^{1/2} / d_{ab} \quad (5)$$

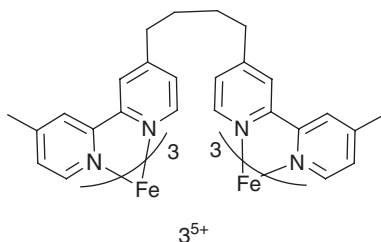
which is the form usually used by experimentalists.^{11,45}

The classical two-state Hamiltonian has been widely used by scientists. It is, for example, the same one that was classically used for the motion of planets (with elliptic diabatic orbitals instead of parabolic ones). One could easily imagine that there might be problems applying classical theory to the motion of electrons within

molecules, and even more with carrying out classical analysis of absorption spectra. Furthermore it is now accepted that ET is a tunneling process that must be treated quantum mechanically, and so that the system never goes through the transition state that lies ΔG^* above the ground state.¹⁶ This chapter will discuss ET reactions in all-organic, symmetric *IV* systems that are radical cations with dinitrogen **M** groups. These studies were the first that allowed measurement of the rate constant for ET using electron spin resonance (ESR) in systems for which $\Delta G^\circ = 0$, where it is unambiguously known, and for which the optical spectrum allows independent estimation of ET parameters. The experiments provide stringent tests of ET theory, as will be described below.

2 Determination of k_{ESR} values for σ -bridged systems

When we realized that although Marcus–Hush (MH) theory allows prediction of thermal ET rate constants from the optical spectra of symmetrical *IV* compounds, but no such rate constants had ever been measured, we decided to try to determine them. Making such measurements is actually rather difficult. First, because ΔG° for ET is zero, a symmetrical *IV* compound is always at equilibrium, so there is no transient to follow. About the only way to tell that ET has occurred is to use some sort of lifetime-dependent spectral line broadening technique. Another reason the experiment is difficult is that the metal coordination compounds which are used as the charge-bearing units of *IV* compounds have rather small reorganization energies λ , making ET barrier too small to determine by most methods. Furthermore, as shown in Equations (4) and (5), the intensity of the *IV* band drops to zero as V_{ab} decreases, so it is difficult to observe it for small V_{ab} compounds. Elliott and co-workers reported the first experimentally determined metal-centered symmetrical *IV* compound rate constants in 1998.¹⁷ They studied the very small λ_{v} (argued to be negligible) but rather large distance (Fe–Fe distance estimated at 8.9(2) Å) dinuclear tris(2,2'-bipyridine)iron complex 3^{5+} .



Marcus pointed out that λ consists of two additive components, the solvent reorganization energy, λ_{s} , which increases with distance between the **M** groups, and the internal vibrational one (λ_{v}), which is determined by the **M** groups. The relatively large distance makes λ_{s} large enough that the *IV* band maximum ($\bar{\nu}_{\text{max}} = \lambda$ using MH theory) is 7470 cm^{-1} ($21.4\text{ kcal mol}^{-1}$); 3^{5+} has only a tiny *IV* ϵ_{max} of

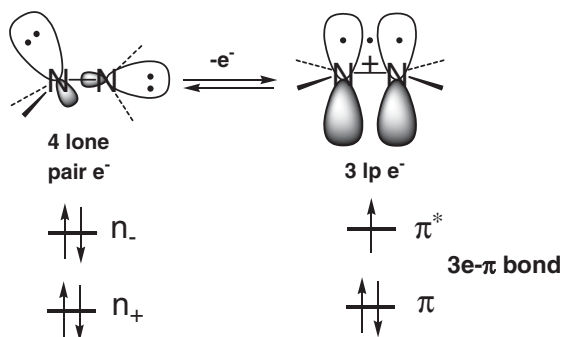
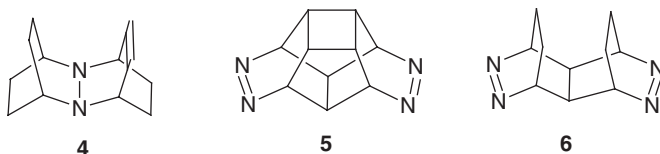


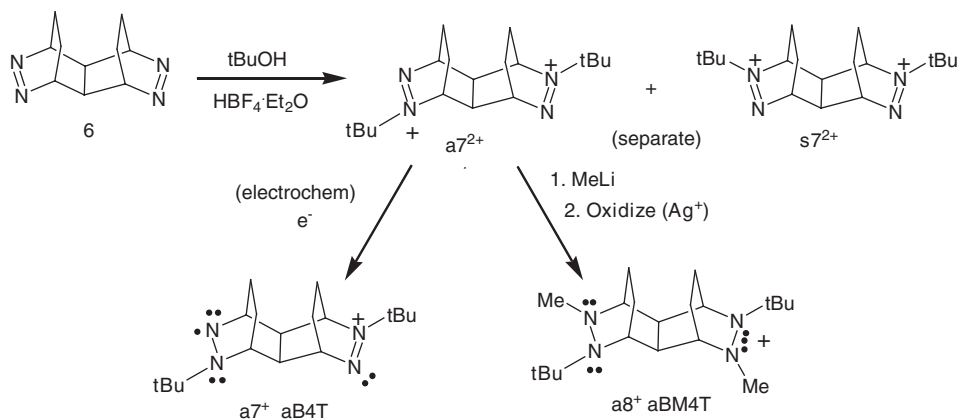
Fig. 3 Geometry change upon electron loss from hydrazines.

$0.24(1) \text{ M}^{-1} \text{ cm}^{-1}$,¹⁸ which results in rate constants between $4.9(2) \times 10^5 \text{ s}^{-1}$ at 230 K and $7.1(6) \times 10^6 \text{ s}^{-1}$ at 303 K, which were determined by nuclear magnetic resonance (NMR) line broadening.

We had intensively studied ET reactions between neutral hydrazines and their radical cations, and demonstrated that hydrazines exhibit exceptionally large geometry changes upon electron removal, as indicated in Fig. 3. Neutral hydrazines have strongly pyramidal nitrogens and electronically prefer perpendicular lone-pair orbital axes.¹⁹ The NN bond distance contracts about 0.1 Å upon electron removal,²⁰ and hydrazine radical cations have flattened nitrogens and a strong electronic preference for coplanar lone-pair orbital axes.²¹ The large geometry change upon electron loss for hydrazines results in exceptionally large and substituent-dependent λ_{v} values for them, as demonstrated by studies of self-exchange reactions between tetraalkylhydrazines and their radical cations. Self-exchange ET for tetraalkylhydrazines with their radical cations only have second-order rate constants large enough to be accurately measurable by NMR line broadening (second-order rate constants over about $10^3 \text{ M}^{-1} \text{ s}^{-1}$) when the neutral forms are restricted to have the lone pair, lone pair twist angle θ far from 90° , as is the case for the unsaturated bis(*N,N'*-bicyclic) **4**^{0/+},^{22–24} and several examples with other ring sizes.^{25,26}

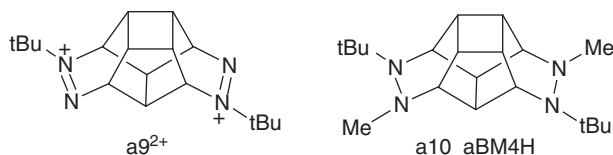


We had therefore decided to obtain measurable ET rate constants by having high λ values and moderately large V_{ab} instead of using the very small V_{ab} value approach that Elliott and coworkers employed for their small λ transition metal-centered **M** groups. We made dinitrogen-centered *IV* compounds from bis(azo) compounds that have such large λ values that V_{ab} can be large enough that the *IV* band ϵ_{max} is high enough for convenient study. Preparation of the hexacyclic 4- σ -bond-bridged bis(azo) compound **5** from cyclooctatetraene had been reported by Shen in 1971,²⁷



Scheme 1 Conversion of bis(azo) compound **6** to bis(trialkyldiazonium) radical cation **7⁺** and bis(tetraalkylhydrazine) radical cation **8⁺** IV compounds.

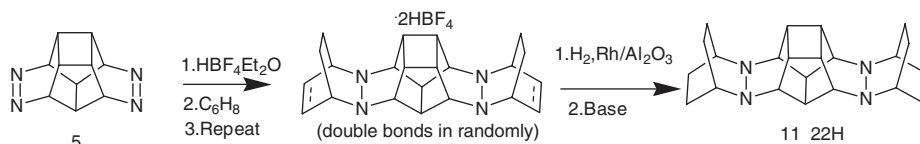
and catalytic reduction of an intermediate two steps before this bis(azo) compound allowed preparation of its tetracyclic analog **6** by the same route.²⁸ As shown in Scheme 1, bis(*tert*-butylation) of the bis(azo) compounds produces 1:1 mixtures of *syn* and *anti* bis(trialkyldiazonium) dications, each of which can be converted to two IV compounds. Simple reduction gives a bis(diazonium) monocation, which has a paramagnetic trialkylhydrazyl neutral dinitrogen unit, and a diamagnetic trialkyldiazonium cationic dinitrogen unit. Addition of methyllithium produces the *tert*-butyl methyl hydrazine, which can be oxidized with silver cation to an IV radical cation that has the paramagnetic dinitrogen unit cationic and the diamagnetic one neutral. Similar chemistry was used to prepare the isomers of **9²⁺** but they proved harder to separate and only the *anti* isomer was obtained pure enough for study. The corresponding *anti* hexacyclic-bridged IV bis(hydrazine) precursor, **a10** was prepared from **5** in the same manner.²⁹ The optical and ESR results for these



4- σ -bond-bridged IV compounds are summarized in Table 2. This work established that organic-centered Class II IV compounds had broad, Hush-type absorption bands like the previously studied metal-centered examples. The ESR spectra of these compounds showed that the bis(diazoniums) had ET that was too fast to measure by ESR and that the bis(hydrazines) had ET that was too slow. The ESR method only allows study of a narrow range of rate constants near the point of maximum broadening, which corresponds to the ESR splitting constant being observed in MHz units, or near 10^8 s^{-1} for the nitrogen splitting of both bis(hydrazine) and bis(diazonium)

Table 2 Optical data for 4- σ -bond-bridged *IV* compounds in acetonitrile²⁹

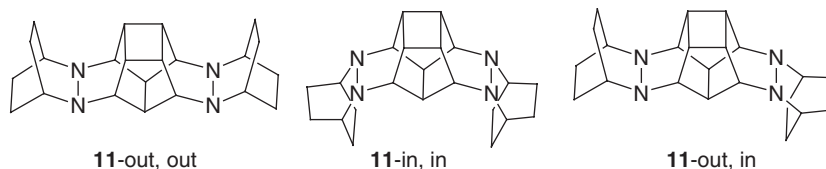
| Compound | M | $\bar{\nu}_{\max}^a$ | ϵ_{\max}^b | $V_{ab}^{a,c}$ | k_{ESR} |
|--------------------------------------|-----------|----------------------|---------------------|----------------|------------------|
| s7 ⁺ sB4 T ⁺ | Diazenium | 10,600 | 610 | 1270 | Too fast |
| a7 ⁺ aB4 T ⁺ | Diazenium | 10,900 | 560 | 1050 | Too fast |
| a9 ⁺ sB4 H ⁺ | Diazenium | 12,000 | 540 | 1150 | Too fast |
| s8 ⁺ sBM4 T ⁺ | Hydrazine | 19,500 | 1450 | 1350 | Too slow |
| a8 ⁺ aBM4 T ⁺ | Hydrazine | 19,400 | 940 | 1370 | Too slow |
| a10 ⁺ aBM4 H ⁺ | Hydrazine | 18,250 | 1350 | 1180 | Too slow |

^acm⁻¹.^bM⁻¹ cm⁻¹ (assuming 100% yield of radical ion from the precursor).^cUsing Equation (3) with d_{ab} as the calculated shortest through-bond N,N distance.**Scheme 2** Preparation of **11**.

radical cations. These methyl-substituted hydrazines were also rather unstable, and decomposition could be detected while the measurements were being made. The bis(diazeniums) showing k_{ESR} too fast to measure and bis(hydrazines) too slow is what is expected from Marcus theory, equating $\bar{\nu}_{\max}$ with λ and using Equation (4) for ΔG^* . It was obvious that we had to either increase k_{ESR} for hydrazine-centered compounds or decrease it for the diazenium-centered ones, and we set out to do both.

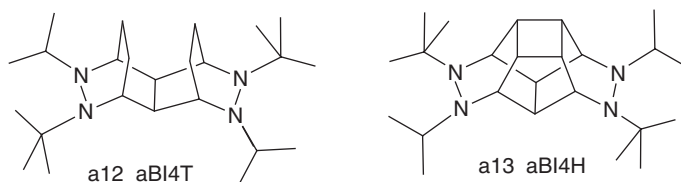
We decided that what we needed to make was **11**⁺. We estimated from the self-exchange studies²³ and semiempirical calculations of λ_v^{24} that this compound would have a k_{ESR} value in the right range for measurement, and bis(*N,N'*)bicyclic hydrazines were known to be isolable as radical cations, so the decomposition difficulties encountered for the *N*-methylhydrazines should also disappear. Furthermore, we had a preparation that gave the bis(bicyclic) hydrazine **M** group of **11** in 93% yield from the monoazo compound,³⁰ so we expected the chemistry to be easy (once the known bis(azo) compound was obtained). This proved incorrect, and it took us over 15 person-years to make **11** because everything possible went wrong (see Scheme 2). First, the bis-adduct had to be prepared by repeated addition of tiny aliquots of acid and cyclohexadiene to the bis(azo) compound, because the diprotonated material polymerized cyclohexadiene more rapidly than it added to it. Then, the retro-Diels–Alder reaction took place so rapidly upon deprotonation of the bis-adduct that a means of hydrogenating the protonated adduct had to be developed. It was, by Yichun Wang, who was working on entirely different projects.³¹ Upon obtaining **11**, we were indeed rewarded by **11**⁺ being stable and having the predicted rate constant at room temperature. However, it proved to have an anomalously small temperature coefficient for ET, which certainly cannot be explained by MH theory.³² After considerable agonizing about what might be happening, we suggested that it is probably

an unanticipated conformational problem.³³ The dissymmetry of the bridge makes it have two faces. We thought that one face would be less hindered than the other, and expected **11** to exist in the out,out double nitrogen inversion form that calculations predict to be most stable. For example, MM2, AM1, and



B3LYP³⁴ calculations all get **11-out,out** to be most stable, **11-in,out** next, and **11-in,in** highest in enthalpy. However, ¹³C-NMR studies showed that solutions of **11** at 230 K are 90% **11-in,out** and only 10% a symmetrical isomer that we presume is **11-out,out**. There is a 13.2(6) kcal mol⁻¹ barrier to interconversion of the **in** and **out** rings for **11-in,out** significantly higher than the 10.4 kcal mol⁻¹ barrier for double nitrogen inversion in its monohydrazine analog. If the radical cation is also unsymmetrical, ET would lead to a higher-energy form, and because of the great sensitivity of ET to driving force, the equilibrium constant for formation of a symmetrical form would appear in the observed rate constant for intramolecular ET. We cannot confirm this experimentally, but both AM1 and UHF/6-31G* calculations get the result that **11⁺-in,out** is the most stable of the three conformations.^{34b} Unrestricted Hartree-Fock (UHF) calculations overestimate flattening in hydrazine radical cations, and as a result give poor calculated λ values even though their NN distances are far better than those of AM1 calculations. Quite expensive calculations would have to be done to more reliably estimate the relative energies of the conformations of **11**. After we switched to studying bis(*anti* hydrazines) instead of this bis(*syn*) one, the anomalous temperature coefficient was not observed again, so the problem seems indeed to be associated with the bis(*syn*) conformations of **11**.

Ling-Jen Chen discovered that isopropyl groups are effective both at lowering barriers for double nitrogen inversion (which means that λ_v will be lower) and at stabilizing the radical cations,³⁵ so we next switched to study the *N*-isopropyl analogs of **8** and **10**, which are **12** and **13**. They were indeed more stable, and had large enough ET rate constants to be measured by ESR.³⁶ The activation parameters obtained are summarized in Table 3, along with the data for **11⁺**. No one thinks that the Eyring pre-exponential factor ($k_b T/h$) is suitable to use for interpretation of ET reactions, so the ΔS^\ddagger values are



somewhat arbitrary, but the statistical scatter shown is convenient to compare with other rate constant measurements. The ΔH^\ddagger values obtained for these *anti* alkylated

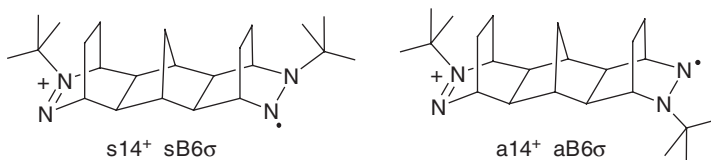
Table 3 Eyring activation parameters and extrapolated ESR rate constants for 4- σ -bond-bridged bis(hydrazine) *IV* radical cations

| Compound | Solvent | <i>T</i> range | $\Delta H^{\ddagger a}$ | $\Delta S^{\ddagger b}$ | $k_{\text{ESR}}^c(298)$ |
|---------------------------------|--------------------------|----------------|-------------------------|-------------------------|-------------------------|
| 11^+ 22H^+ | CH_3CN | 250–350 | 0.66 (13) | –19.2 (4) | 1.32 (4) |
| $a12^+$ $a\text{BI}4\text{T}^+$ | CH_2Cl_2 | 264–304 | 3.0 (6) | –11.8 (21) | 1.05 (7) |
| $s12^+$ $s\text{BI}4\text{T}^+$ | CH_2Cl_2 | 264–304 | 3.3 (3) | –10.9 (10) | 0.96 (3) |
| $a13^+$ $a\text{BI}4\text{H}^+$ | CH_2Cl_2 | 283–308 | 4.0 (7) | –8.2 (22) | 1.24 (4) |

^akcal mol^{–1}.^bcal mol^{–1}deg^{–1}.^c10⁸ s^{–1}.

bis(hydrazines) are 3–4 kcal mol^{–1}, which is much more reasonable for a single-step ET process than the 0.7 kcal mol^{–1} obtained for 11^+ . Because the *syn* and *anti* conformations appear to have the same ET parameters, the principal value of studying both is to provide truly independent samples to estimate the errors involved in the measurements.

To enable measurement of k_{ESR} for bis(diazonium) radical cations, it was necessary to decrease V_{ab} , so we synthesized the 6-bond-bridged systems **14** and **15**, which required first making the 6-bond-bridged bis(azo) compound. They indeed have slow enough



ET to measure by ESR, and their activation parameters are summarized in Table 4.³⁷ Their ΔH^{\ddagger} values are slightly higher than those of the 4- σ -bond-bridged bis(hydrazines), but their ΔS^{\ddagger} values are significantly less negative.

3 Determination of k_{ET} values for π -bridged systems

Changing the bridge for the σ -bridged compounds discussed above requires preparation of a different bis(azo) compound, which is a tedious process. We began to make more rapid progress when we realized that a series of π -bridged systems with 2-*tert*-butyl-2,3-diazabicyclo[2.2.2]oct-2-yl (**15**, which we abbreviate **Hy**) **M** units could be

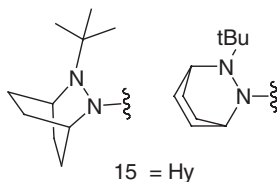
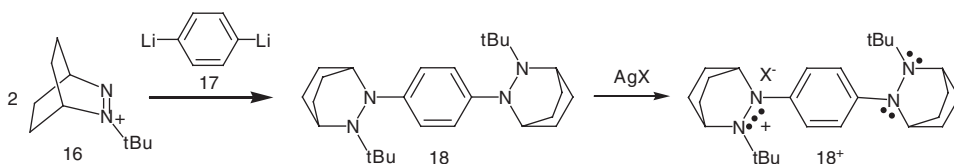


Table 4 Eyring activation parameters and extrapolated ESR rate constants for 6- σ -bond-bridged bis(diazenium) *IV* radical cations

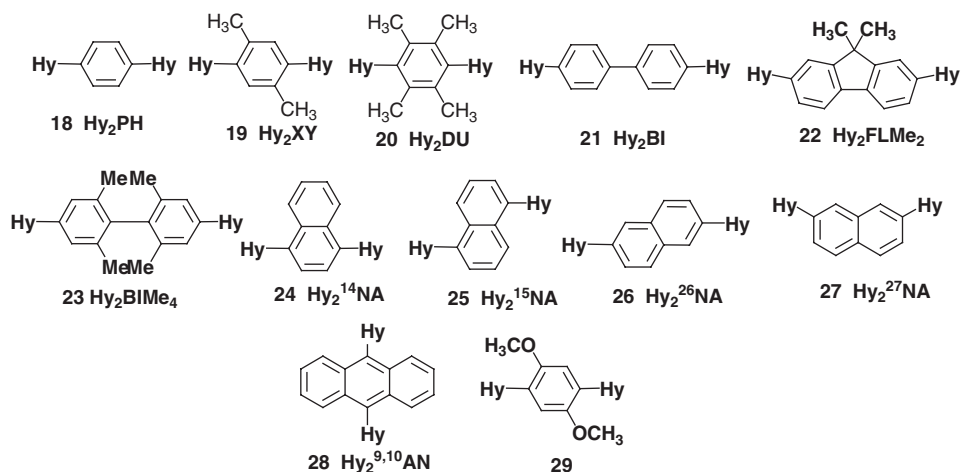
| Compound | Solvent | <i>T</i> range | $\Delta H^{\ddagger a}$ | $\Delta S^{\ddagger b}$ | $k_{\text{ESR}}^c(298)$ |
|---------------------------------|---------------------------------|----------------|-------------------------|-------------------------|-------------------------|
| S14 ⁺ sB6 σ^+ | CH ₃ CN | 273–323 | 4.5 (6) | –6.5 (20) | 1.14 (7) |
| a14 ⁺ aB6 σ^+ | CH ₃ CN | 284–334 | 4.3 (4) | –6.6 (22) | 1.04 (9) |
| S14 ⁺ sB6 σ^+ | PrCN | 263–313 | 4.3 (4) | –7.2 (14) | 1.22 |
| a14 ⁺ aB6 σ^+ | PrCN | 263–313 | 4.5 (4) | –6.4 (12) | 1.25 |
| S14 ⁺ sB6 σ^+ | DMF | 283–333 | 4.8 (6) | –6.5 (20) | 0.77 (5) |
| a14 ⁺ aB6 σ^+ | DMF | 283–343 | 4.6 (4) | –7.1 (12) | 0.79 (4) |
| S14 ⁺ sB6 σ^+ | DMSO | 293–333 | 4.4 (4) | –7.6 (12) | 0.78 |
| a14 ⁺ aB6 σ^+ | DMSO | 293–334 | 4.2 (3) | –8.4 (11) | 0.82 |
| S14 ⁺ sB6 σ^+ | CH ₂ Cl ₂ | 214–293 | 4.0 (11) | –6.5 (43) | 2.7 (+13, –10) |
| a14 ⁺ aB6 σ^+ | CH ₂ Cl ₂ | 214–293 | 3.6 (10) | –8.4 (42) | 2.2 (+11, –8) |

^akcal mol^{–1}.^bcal mol^{–1}deg^{–1}.^c10⁸ s^{–1}.**Scheme 3** Preparation of **18⁺** from trialkyldiazonium cation **16** and 1,4-dilithiobenzene.

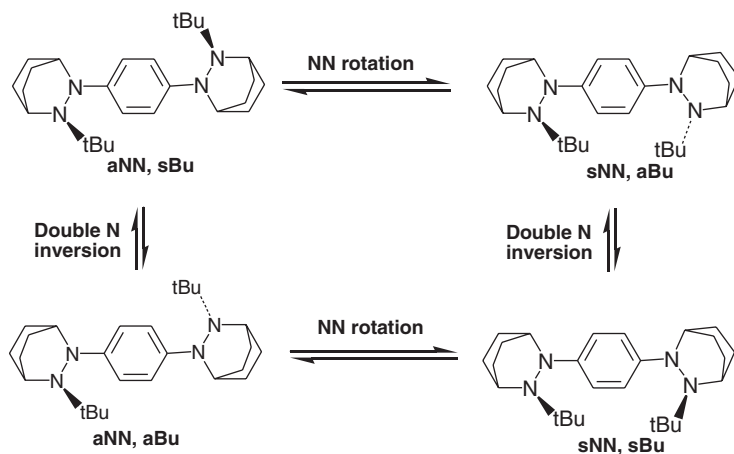
prepared by coupling 2-*tert*-butyl-2,3-diazabicyclo[2.2.2]oct-2-ene cation (**16**) to dilithioaromatics, as shown in **Scheme 3** for the parent.

The structures of a dozen such compounds we studied appear in **Scheme 4**. We initially prepared **18⁺** because AM1 calculations get the result that it is localized. Although we believe it is naive to consider that such calculations can predict such a subtle property accurately, **18⁺** is localized, as shown both by its broad Hush-type *IV* band and its ESR spectrum at -105° in 12:1 acetone:acetonitrile, which exhibits the broadened pentet expected for only two equivalent nitrogens sharing the charge on the ESR timescale.³⁸ Since **18⁺** (**Hy₂PH⁺**) showed ET that was too rapid for quantitative ESR measurements in pure solvents, we switched the aromatic ring to *p*-xylene-2,5-diyl (**19⁺**) and durene-1,4-diyl (**20⁺**).³⁹ As expected, the methyls force greater twist at the C_{Ar}–N bonds, and since V_{ab} is approximately proportional to the cosine of the twist angle at each C_{Ar}–N bond,¹⁵ k_{ET} is smaller, and is in the measurable range.

Scheme 5 illustrates the conformational complexity which is built into symmetrical *IV* compounds that have unsymmetrical **M** groups attached to symmetrical bridges by single bonds. Rotation about these bonds interconverts *syn* and *anti* conformations of the **M** groups. For these compounds, double nitrogen inversion also interconverts *syn* and *anti tert*-butyl group conformations, so there are four diastereomeric conformations of **18**. All are present in equal amounts for neutral **18**,



Scheme 4 Neutral forms of Hy_2Ar^+ studied for ET properties.



Scheme 5 Interconversion of diastereomeric conformations of **18**.

as demonstrated by ^{13}C -NMR, so one hydrazine unit is not affected by the configuration of the other one. Calculations indicate that the same is true for the radical cations, and we have no evidence that this conformational complexity affects intramolecular ET rates in these compounds.

Expanding the number of linking bonds from the five of **18–20** to nine decreases V_{ab} , and the biphenyl-bridged compound (**21**⁺) does not need flanking methyl groups to give a measurable k_{ESR} .^{40,41} Since biphenyl is twisted at the central CC bond, we expected the untwisted 9,9-dimethylfluorene-2,7-bridged compound **22**⁺ to have faster ET, which it does. Flanking the central bond with methyl groups in **23**⁺ greatly slows ET, and we could neither observe any line broadening for

intramolecular ET by ESR or see any appreciable absorption where the IV band for 21^+ and 22^+ appears. The 1,4-naphthalene-bridged compound 24^+ has an ET rate constant close to that for the xylene compound, and a rather similar calculated C_{Ar-N} twist angle.⁴⁰ The 2,6-substituted compound (26^+ , which is 7-bond-bridged instead of five) has a rather comparable rate constant, but the 1,5-substituted one (25^+ , 5-bond-bridged) shows far slower ET, while the 2,7-substituted 27^+ (6-bond-bridged) shows no ESR broadening corresponding to ET, and has only very small IV absorption.⁴² These results make it clear that the great emphasis upon ET distance in the literature has been somewhat misplaced. V_{ab} does correlate with the number of bonds and hence distance when 1,4-substituted benzenes and double and triple bonds are linked, but does not correlate at all when positions of substitution on aromatic rings are changed.

The 9,10-anthracene-bridge compound 28^+ has a very similar twist angle to the durene-bridged 20^+ , but exhibits a far faster k_{ESR} value, comparable to 18^+ .⁴³ Obviously, some new factor is involved in its ET as is revealed by its optical spectrum, and will be discussed below (Section 9). In contrast to the *p*-xylene-bridged 19^+ , the dimethoxybenzene-bridged 29^+ also exhibits ET that is too fast to measure by ESR.⁴⁴

The activation parameters obtained from the rate constants determined by ESR for π -bridged bis(hydrazines) are summarized in Table 5.

Table 5 Eyring activation parameters and extrapolated ESR rate constants for aryl-bridged bis(hydrazine) IV radical cations

| Compound ^a | Solvent ^b | T range | $\Delta H^{\ddagger c}$ | $\Delta S^{\ddagger d}$ | $k_{ESR}^e(T, K)$ | $k_{ESR}^e(T, K)$ | Ref. |
|-----------------------|----------------------|-----------|-------------------------|-------------------------|-------------------|-------------------|------|
| 19^+ (5) | AN | 236–255 | 2.81 (4) | –9.2 (2) | 2.30 (260) | 5.2 (298) | 39 |
| Hy_2XY | MC | 187–212 | 2.65 (25) | –6.7 (13) | 11.0 (260) | 24 (298) | 39 |
| 20^+ (5) | AN | 236–265 | 4.76 (24) | –1.8 (10) | 2.18 (260) | 8.1 (298) | 39 |
| Hy_2DU | MC ₂ | 183–213 | 3.21 (11) | –4.1 (5) | 14.1 (260) | 36 (298) | 39 |
| 21^+ (9) | AN | 328–353 | 3.48 (13) | –10.9 (4) | 0.26 (260) | 0.71 (298) | 40 |
| Hy_2BI | MC ^f | 263–278 | 3.65 (43) | –7.0 (16) | 1.37 (260) | 3.86 (298) | 41 |
| | MC ^g | 278–303 | 3.13 (15) | –9.8 (5) | 0.89 (260) | 2.21 (298) | 41 |
| 22^+ (9) | AN | 248–273 | 3.95 (9) | –5.5 (4) | 1.59 (260) | 4.84 (298) | 40 |
| Hy_2FLMe_2 | MC ^g | 218–238 | 2.61 (9) | –9.0 (4) | 3.77 (260) | 8.82 (298) | 41 |
| 24^+ (5) | Ace | 188–228 | 1.70 (14) | –12.6 (7) | 1.5 (215) | 3.85 (260) | 40 |
| $Hy_2^{14}NA$ | AN | 223–243 | 2.28 (27) | –9.9 (11) | 4.45 (260) | 8.95 (298) | 42 |
| 25^+ (5) | DCE | 303–338 | 4.7 (3) | –6.6 (9) | 0.027 (215) | 0.83 (298) | 42 |
| $Hy_2^{15}NA$ | | | | | | | |
| 26^+ (7) | MC | 193–218 | 1.8 (4) | –10.9 (21) | 2.8 (215) | 7.40 (260) | 42 |
| $Hy_2^{26}NA$ | Ace | 213–248 | 2.8 (2) | –9.0 (8) | 0.69 (215) | 2.78 (260) | 42 |

^aThe number in parenthesis is the number of bonds between the hydrazine units.

^bSolvents – Ace: acetone; AN: acetonitrile; DCE: 1,2-dichloroethane; MC: methylene chloride.

^ckcal mol^{–1}.

^dcal mol-deg^{–1}.

^e10⁸ s^{–1}.

^fConcentration as low as feasible (0.19 mM), to minimize ion pairing.

^gWith 20 mM added Bu₄N⁺ PF₆[–], to maximize ion pairing.

4 Determination of ET parameters from the *IV* band

Several issues have to be addressed before quantitative comparisons between the rate constants discussed above and the optical spectra observed for these compounds can be made.

IV BANDWIDTH

Classical analysis of the two-state model using parabolic diabatic surfaces produces a Gaussian-shaped *IV* band having a full-width at half-maximum intensity that is only determined by $\bar{\nu}_{\max}$.^{14,55}

$$\Delta\bar{\nu}_{1/2}(\text{HTL}) = [(16 \ln(2)k_{\text{b}}T)\bar{\nu}_{\max}]^{1/2} \quad (6)$$

Experimentally Class II *IV* compounds show bands that are broader than $\Delta\bar{\nu}_{1/2}(\text{HTL})$ and usually have the high-energy half-width at half-height slightly broader than the low-energy one. Hush rationalized this effect using an ET parameter that does not appear in a classical analysis, but is important for newer ET theory,⁸ the energy of the barrier-crossing frequency, ω_{v} (which is also called $h\nu_{\text{v}}$; we use cm^{-1} as the units of the ET energy parameters in this discussion; some people use the symbol ω only for the frequency, units s^{-1}). The HTL of Equation (6) stands for the classical *high-temperature limit*, which is only reached when $2k_{\text{b}}T$ ($= 452 \text{ cm}^{-1}$ at 25°C) is $> \omega_{\text{v}}$, which is not the case for organic charge-bearing units.

The *X*-axis for the MH classical two-state model (Fig. 2) includes the effects of both solvent and internal reorganization. We can see no reason to expect that these diabatic surfaces would be perfect parabolas, and pointed out that if the requirement that the diabatic surfaces be perfect parabolas is relaxed and a quartic term is added so that the diabatic surfaces are given by:⁴⁶

$$\begin{aligned} H'_{\text{aa}} &= [\lambda X^2/(1+Q)][1+QX^2] \\ H'_{\text{bb}} &= [\lambda(1-X)^2/(1+Q)][1+Q(1-X)^2] \end{aligned} \quad (7)$$

The observed *IV* bands are fit as well with two parameters (λ and Q) using classical theory as they are by using the far more complex four parameter Bixon–Jortner¹⁶ (BJ) approach (see Section 8) that uses an additional parameter (λ_{s} , λ_{v} , and ω_{v}), which was first applied to fitting absorption spectra quantitatively by Ralph Young of the Kodak group.⁴⁷ Observed bandwidth (the Q value required to fit the *IV* band) clearly depends upon solvent, so bandwidth is not an experimental measure of ω_{v} , as was suggested.¹⁵ The $(1+Q)^{-1}$ multiplier in the first term provides normalization, which keeps $\bar{\nu}_{\max}$ close to the classical MH definition of λ ; a significantly greater increase in $(\lambda_{\text{v}} + \lambda_{\text{s}})$ over $\bar{\nu}_{\max}$ occurs using the BJ approach. When $Q > 0$ the diabatic curves no longer cross at $\lambda/4$, and complete solutions using Equation (7) as the diabatic surfaces produce ΔG^* values that are within experimental error of the result using the parabolic diabatic surface ΔG^* , Equation (3) with the curve-crossing point $\lambda/4$ term replaced by the curve-crossing point for

quartic surfaces, $[(1 + Q/4)/(1 + Q)]\lambda/4$. The corresponds to $0.875\lambda/4$ at $Q = 0.2$, as is observed in methylene chloride for some *IV* compounds that we have studied.

Because the *IV* bands are slightly distorted from Gaussian, we have also examined calculating V_{ab} using the transition dipole moment (μ_{12}) instead of the Gaussian approximation. Liptay pointed out that the proper equation for calculating μ_{12} is:⁴⁸

$$\mu_{12} = \frac{1000 \ln(10) 3hc}{8\pi^3 N_A} \left[\int_{\text{band}} \frac{\varepsilon(\bar{\nu})}{\bar{\nu}} d\bar{\nu} \right]^{1/2} = 0.09584 \left[\int_{\text{band}} \frac{\varepsilon(\bar{\nu})}{\bar{\nu}} d\bar{\nu} \right]^{1/2} \quad (8)$$

It allows obtaining proper values even for complex bands that show vibrational fine structure. The values obtained do not differ substantially from using a Gaussian approximation, but it should be pointed out that if a band is simulated as a sum of Gaussians, the μ_{12} for the band is smaller than the sum of the μ_{12} values for the individual Gaussians.

A more important change was introduced by Ralph Young of the Kodak group. Both the Hush equations (4) and (5) and the Liptay equation (8) are correct for the gas phase, but experiments on *IV* compounds are conducted in solution. Various ways of accounting for the fact that μ_{12} values depend slightly upon solvent have been suggested. The one that we employ here is what Young and coworkers⁴⁹ call the Chako⁵⁰ factor, which is the square root of what Calvert and Pitts⁵¹ call the Rubinowicz factor.⁵² The effect of this refractive index (n) correction is to multiply μ_{12} (and hence V_{ab}) by a factor f as shown below:

$$f = 3(n)^{1/2}/(n^2 + 2) \quad (9)$$

This f correction corresponds to a factor of 0.914 for acetonitrile and 0.890 for methylene chloride at 298 K. Its use usually brings the rate constants calculated from the optical spectra (k_{opt}) into better agreement with experimentally measured ones, and we use it in calculating the V_{ab} values used in producing the k_{opt} values discussed in Section 7.

ESTIMATION OF THE ET DISTANCE

There has been considerable confusion in the literature about what the ET distance, the d_{ab} of Equations (2) and (3), actually represents. For transition metal-centered systems the metal–metal distance (estimated from model compounds such as a non-*IV* oxidation level of the compound of interest) was traditionally used as d_{ab} . However, as first pointed out clearly by Cave and Newton in their generalized Mulliken–Hush theory,^{53,54} d_{ab} refers to the diabatic surfaces, while real molecules exist on adiabatic surfaces with electronic couplings intact, so it cannot be directly measured experimentally. Cave and Newton also pointed out that one can convert an ET distance measured on the adiabatic surface, a d_{12} value, to d_{ab} using the optical spectrum with Hush's Gaussian approximation of Equation (3), by employing the following equation:

$$d_{ab} = \left[d_{12}^2 + 4(2.06 \times 10^{-2})^2 \varepsilon_{\text{max}} \Delta\bar{\nu}_{1/2} / \bar{\nu}_{\text{max}} \right]^{1/2} \quad (10)$$

The correction increases as V_{ab}/λ increases, but is relatively small for the compounds discussed here. The question of how to determine d_{12} remains. It is clearly not the distance between any of the atoms in a molecule with organic **M** groups, because the charge and spin are obviously significantly delocalized; d_{12} represents the average distance the electron is transferred as the electron moves between the **M** groups of an *IV* compound along the ET direction. A reasonably general way of obtaining d_{12} is to try to calculate it. Nelsen and Newton suggested using a simple approximation of the following equation:⁵⁵

$$d_{12}(\text{dm}), \text{\AA} = 2\mu_1(\text{Debye})/4.8032 \quad (11)$$

which approximates d_{12} using the calculated dipole moment, μ_1 , at that time employing semiempirical AM1 calculations. Johnson and Hupp used a very similar method, but instead of employing entire calculated dipole moment, used only the point charge contribution to it.⁵⁶ The use of AM1 calculations to compare the d_{12} values of the diastereomeric conformations of *IV* bis(hydrazines) has been described in detail.⁵⁷ An important thing to realize in trying to employ this method is that density functional calculations should not be employed. Their huge overestimation of the stabilization obtained by charge delocalization destroys their ability to describe either the geometry or the charge distribution of *IV* compounds properly.⁵⁸

Boxer introduced using electrooptical (Stark effect) spectroscopy for determining d_{12} of metal-centered *IV* complexes and other ET problems (calling them effective ET distances).⁵⁹⁻⁶³ These methods have also been applied by the groups of Hupp⁶⁴⁻⁶⁸ and of Sutin.^{69,70} We have not had access to the necessary equipment for this experiment, and have used other methods of estimating d_{12} .

We introduced a way of experimentally estimating d_{12} for certain bis(hydrazines), using the diradical dication oxidation level as a model.³⁹ We argued that the average distance between the odd electrons of the triplet state of the dication is close conceptually to the average distance that the electron is transferred in the monocation. Although the singlet is usually the ground state for these compounds, when the triplet is thermally accessible the triplet ESR spectrum can be observed in a glass, and the triplet dipolar splitting in Gauss (D') is related to the average distance between the electrons (d_{ESR}) by:^{71,72}

$$d_{\text{ESR}} = 30.3(D')^{-1/3} \quad (12)$$

Although not available for all compounds we have studied, use of d_{ESR} produces optically calculated rate constants that are closer to experimental ones for 20^+ , 21^+ , and 25^+ than using AM1-calculated $d_{12}(\text{dm})$ to obtain d_{ab} .

5 Ion-pairing effects

Because methylene chloride is a solvent of low dielectric constant, ion pairing occurs detectably even for rather large cations and anions. We will discuss ion-pairing studies involving these compounds before the effects of solvent upon λ , because it is

necessary to deal with ion pairing to establish how λ_s changes. Especially large counterion effects have been found for some experiments on ET within organic compounds, such as in the pulse-radiolytic measurements on $\Delta G^\circ \neq 0$ intramolecular ET reactions by Piotrowiak and Miller.⁷³ They explained these effects using a suggestion by Weaver and coworkers that ion pairing changes the shape of energy wells significantly from being parabolic to having coulombic character.⁷⁴ Ion pairing results in shift of the *IV* band to higher energy, and we have found quantitative agreement with expectation based upon a simple ion-pairing equilibrium as shown below:



Because the band maximum for ion-paired radical cation $\bar{\nu}_{\max}^{\text{IP}}$ is not shifted far from that free radical cation, $\bar{\nu}_{\max}^{\text{free}}$, a simple ion-pairing equilibrium is described by the following equation:

$$\bar{\nu}_{\max} = (\bar{\nu}_{\max}^{\text{free}} + K_{\text{IP}}[X^-]\bar{\nu}_{\max}^{\text{IP}})/(1 + K_{\text{IP}}[X^-]) \quad (14)$$

In Equation (14) $[X^-]$ is the concentration of free X^- , which must be distinguished from the total stoichiometric concentration of X, $X^{\text{tot}} = [X^-] + [AX]$. The equations for fitting experimental data to these equations are given in our first article on this subject.⁴¹ Ion-pairing studies on dithiaspiro-bridged $[\text{Ru}(\text{NH}_3)_5]^{+5}$ systems, biferrocenium cation, and acetylene-bridged biferrocenium have all indicated that simple ion-pairing equilibrium of Equation (13) was not followed. In contrast, we have found excellent agreement with Equations (13) and (14) for our bis(hydrazine) systems, allowing evaluation of the *IV* band maxima for both the free and ion-paired cations, and the energies involved both for ion-pair formation ($\Delta G^\circ_{\text{IP}} = -RT \ln K_{\text{IP}}$), and the increase in free energy for photo-ET between the hydrazine units in the free ion and the ion pair ($\Delta G^\circ_{\text{IP,ET}}(\text{kcal mol}^{-1}) = (\bar{\nu}_{\max}^{\text{IP}} - \bar{\nu}_{\max}^{\text{free}})/350$). The accuracy of K_{IP} measurements (estimated at $\pm 1000 \text{ cm}^{-1}$) from the fitting to plots of $\bar{\nu}_{\max}$ versus total concentration *IV* cation causes errors of about $0.2 \text{ kcal mol}^{-1}$ in $\Delta G^\circ_{\text{IP}}$ and slightly less for $\Delta G^\circ_{\text{IP,ET}}$.⁴¹ Addition of an inert common salt (we studied $\text{Bu}_4\text{N}^+ \text{PF}_6^-$ addition to $\mathbf{20}^+ \text{PF}_6^-$) sets up simultaneous ion-pairing equilibria, allowing determination of K_{IP} for the common salt, which is also included in Table 6. The ion-pairing free energies in CH_2Cl_2 , $\Delta G^\circ_{\text{IP}}$, lie between -4.6 and $-5.3 \text{ kcal mol}^{-1}$ for all the cation, anion pairs, including tetrabutylammonium hexafluorophosphate. The amount that the free energy for vertical ET is increased, $\Delta G^\circ_{\text{IP,ET}}$, is only a fraction of the ion-pairing energy. It obviously depends upon where the counterion is located; if the counterion were exactly symmetrically placed between the hydrazine units, which **M** group had the charge would not be expected to affect λ at all. Obviously counterion position is an ensemble average in solution, where many counterion displacements occur. Because the tetraphenylborates of $\mathbf{18}^+$ and $\mathbf{20}^+$ crystallize without disproportionation and have had their crystal structures determined,³⁹ these crystals provide a unique opportunity to examine how the vertical reorganization energy is affected by 100% ion pairing with a known and specific placement of BPh_4^- counterions. Diffuse reflectance spectra for $\mathbf{20}^+ (\text{Hy}_2\text{DU}^+ \text{BPh}_4^-)$

Table 6 Ion-pairing parameters (at 293 K in CH₂Cl₂)

| Cation | Anion | K_{IP}^a | $\Delta G^\circ_{IP}^b$ | $\nu_{max}^{free\ c}$ | $\bar{\nu}_{max}^{IP\ c}$ | $\Delta G^\circ_{IP,ET}^b$ | Ref. |
|---|-------------------------------|------------|-------------------------|-----------------------|---------------------------|----------------------------|------|
| 20 ⁺ Hy ₂ DU ⁺ | PF ₆ ⁻ | 3100 | -4.7 | 12,400 | 13,100 | +2.0 | 41 |
| 21 ⁺ Hy ₂ BI ⁺ | PF ₆ ⁻ | 3100 | -4.7 | 12,900 | 13,800 | +2.6 | 41 |
| 22 ⁺ Hy ₂ FL ⁺ | NO ₃ ⁻ | 6100 | -5.1 | 11,160 | 12,220 | +3.0 ₅ | 41 |
| 26 ⁺ Hy ₂ ³⁶ NA ⁺ | NO ₃ ⁻ | 3200 | -4.7 | 11,260 | 12,190 | +2.7 | 42 |
| 25 ⁺ Hy ₂ ¹⁵ NA ⁺ | NO ₃ ⁻ | 9700 | -5.3 | 12,460 | 13,510 | +3.0 | 42 |
| 31 ⁺ aBI6σ ⁺ | SbF ₆ ⁻ | 3800 | -4.9 | 17,800 | 18,300 | +1.6 | 76 |
| 34 ⁺ aBP6σ ⁺ | PF ₆ ⁻ | 2200 | -4.6 | 14,300 | 15,100 | +2.2 | 76 |
| Bu4N ⁺ | PF ₆ ⁻ | 6300 | -5.1 | – | – | – | 41 |

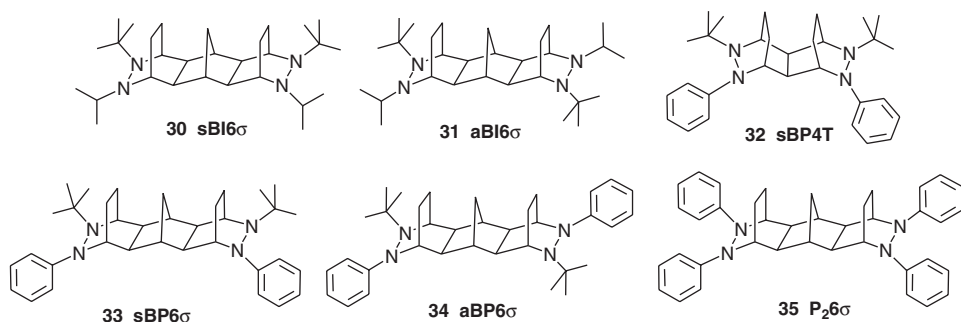
^aM⁻¹.^bkcal mol⁻¹.^ccm⁻¹.

give very similar band shape to solution studies and give $\bar{\nu}_{max}$ of 15,100 cm⁻¹ recorded on an alumina support (slightly higher on LiCl 15,250, BaSO₄ 15,400–15,450, and KBr 15,600).⁷⁵ Solutions in polar solvents show $\bar{\nu}_{max}$ ranging up to 14,700 cm⁻¹ in DMSO and DMF.⁷⁶ The increase in $\bar{\nu}_{max}$ for the solid compared to acetonitrile solution is 1000 cm⁻¹ (2.9 kcal mol⁻¹) compared to an increase of 2900 cm⁻¹ (8.3 kcal mol⁻¹) for **18**⁺ (Hy₂PH⁺BPh₄⁻). The crystal structures rationalize this trend: the counterion for **18**⁺ is less symmetrically placed, lying closer to the oxidized N₂ unit (NN⁺ bond midpoint, B distance 7.01 versus 7.41 Å) than the neutral one (midpoint of NN⁰ unit, B distance 10.76 versus 6.95–7.24 Å for the three diastereomeric conformations present in the crystal). The same principle rationalizes the solution studies. The largest $\Delta G^\circ_{IP,ET}$ values in Table 6 are for **22**⁺ (Hy₂FL⁺) and **25**⁺ (Hy₂¹⁵NA⁺), each of which has the region between the NN bonds sterically encumbered relative to the other compounds, as is experimentally demonstrated for the Hy₂¹⁵NA system by the placement of the counterions in the diradical dication.⁷⁷

The effect of ion pairing on k_{ESR} in methylene chloride was surprisingly small, a factor of 1.5 faster for our most studied system, **21**⁺ (Hy₂BI⁺) under low than high ion-pairing conditions (see Table 5, p. 198). Although k_{opt} rate constant predictions closer to the observed k_{ESR} were obtained when the reaction was assumed to be endothermic by $\Delta G^\circ_{IP,ET}$, even using $\Delta G^\circ = 0$ with parameters obtained from the optical spectrum under the high salt conditions used to maximize ion pairing only increased the k_{opt} prediction by a factor of 2.5.⁴¹

6 Separation of λ_s from λ_v

Medium effects on ET reactions of metal complexes have been recently reviewed.⁷⁸ Measuring the ET rate constant by ESR requires that k_{ESR} be near 10⁸ s⁻¹ at an accessible temperature, but obtaining optical spectra does not, and several systems whose ET rate constants do not lie within the range for which we can measure k_{ESR} have been studied optically⁷⁶ (see Scheme 6 for the structures).



Scheme 6 Neutral precursors of additional bis(hydrazine) radical cations prepared for optical studies.

Solvent effects have been uniquely important in ET studies. Marcus splits the vertical reorganization energy into solvation (often called $\lambda_{o(uter)}$ or $\lambda_{s(olvent)}$) and internal (often called $\lambda_{i(nner)}$ or $\lambda_{v(ibrational)}$) components using dielectric continuum theory and introduced using the following equation to predict λ_s :

$$\lambda_s = e^2 g(r, d) \gamma \quad (15)$$

The solvent-dependent term is $\gamma = 1/n^2 - 1/\epsilon_s$, sometimes called the Pekar factor,⁷⁹ where n is the refractive index of the solvent and ϵ_s is the static dielectric constant.⁷ The $g(r, d)$ is a distance term having units of \AA^{-1} , depending upon various degrees of sophistication⁸⁰ on the distance between the charge-bearing units, and e^2 (in the energy and distance units used in this chapter) is $1.161 \times 10^5 \text{ cm}^{-1} \text{ \AA}$. Many quantitative experimental studies have relied upon this simple theory to separate λ_s from λ_v ,⁸⁰ which is especially necessary for rate constant prediction using the more modern BJ theory.¹⁶ Furthermore, because of the narrow dynamic range of ESR measurements of k_{ET} , we have often used methylene chloride as a solvent, because it gives larger k_{ESR} by a factor of about five than acetonitrile, and it also has both good solubility for our compounds and a low-melting point, so experiments can be conducted at much lower temperatures than in most more polar solvents. We therefore felt it was important to be able to separate λ_s from λ_v for *IV* bis(dinitrogen) cations.

Dielectric continuum theory obviously cannot separate λ_s from λ_v for bis(dinitrogen) radical cations, because plots of \bar{v}_{max} ($= \lambda$) versus γ for them are far from being linear. There is an obvious effect that correlates with solvent donicity, because good donor solvents like DMF and DMSO have larger \bar{v}_{max} values than acetonitrile, which has a larger γ value. We have found that for the rather limited set of solvents that we have employed, \bar{v}_{max} can be converted to a linear relationship with γ using the following relationship:

$$\bar{v}_{cor} = A + B\gamma + C(DN) \quad (16)$$

where A , B , and C are adjusted fitting parameters, and DN is the Gutmann donicity number,⁸¹ which is the absolute value of the heat of mixing of a solution of $SbCl_5$ in 1,2-dichloroethane (DCE) with another solvent, so $DN \equiv 0$ for DCE (and we used it

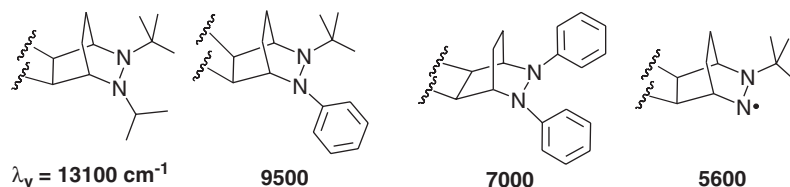
as zero for methylene chloride also) and increases with the heat of mixing. Methylene chloride was only included in the correlation when $\bar{\nu}_{\max}^{\text{free}}$ was available, because otherwise the observed value includes effects of ion pairing. Similarly, other low enough polarity solvents (benzonitrile, pyridine) were excluded for the same reason, but from the sizes of the K_{IP} values measured in methylene chloride and the known dependence of ion pairing on ϵ_{S} , we expect measurements in acetone, butyronitrile, DMF, and DMSO to require no adjustment and we used these data to determine the fitting constants. Both B and C are solvent dependent, but A is not, and we equate A with λ_{v} . Data for which solvent studies of this sort have been done are summarized in Table 7.

The “rms fit” values of Table 7 are small enough compared to our estimated $\pm 100 \text{ cm}^{-1}$ accuracy of measuring $\bar{\nu}_{\max}$ to call $\bar{\nu}_{\text{cor}}$ linear with γ . Although we do not believe it can be stated that solvent donicity “causes” the changes in $\bar{\nu}_{\max}$ that are observed, use of the three-parameter Equation (17) produces A values that we argue are close to λ_{v} because of their dependence upon structure of the IV compound. As shown in Scheme 7, the λ_{v} values obtained in Table 7 for similar structural units are

Table 7 Separation of λ_{v} from λ_{s} (cm^{-1}) using Equation (13)

| Cation from | $A = \lambda_{\text{v}}$ | B | C | rms fit ^a | λ_{s} MeCN |
|-------------------------------------|--------------------------|--------|-----|----------------------|---------------------------|
| 11 22H | 14,300 | 3800 | -3 | 41 | 1990 |
| 12sBI4T | 13,050 | 6810 | 93 | 60 | 4930 |
| 30 sBI6 σ | 13,130 | 12,100 | 109 | 71 | 7940 |
| 31 aBI6 σ | 13,110 | 12,150 | 196 | 60 | 7900 |
| 32 sBP4T | 9450 | 8180 | 68 | 52 | 5280 |
| 33 sBP6 σ | 9330 | 12,970 | 113 | 98 | 8430 |
| 34 aBP6 σ | 9770 | 11,870 | 97 | 45 | 7620 |
| 35 P26 σ | 6960 | 6530 | 58 | 24 | 4230 |
| 18 Hy ₂ PH | 9810 | 5600 | 31 | 21 | 3390 |
| 20 Hy ₂ DU | 10,100 | 5800 | 69 | 65 | 4020 |
| 25 Hy ₂ ¹⁵ NA | 9920 | 6660 | 65 | 46 | 4400 |
| 26 Hy ₂ ³⁶ NA | 9900 | 3520 | 100 | 85 | 3400 |
| 21 Hy ₂ BI | 9500 | 9100 | 70 | 55 | 5770 |
| 14 sB6 σ^{2+} | 5610 | 11,960 | 86 | 29 | 7520 |
| 14 sB6 σ^{2+} | 5530 | 12,080 | 87 | 25 | 7590 |

^aThe “rms fit” column of Table 7 is the root mean square vertical deviation of the $\bar{\nu}_{\text{cor}}$ versus γ line from a linear regression through the points.



Scheme 7 λ_{v} values obtained from optical studies on σ -bridged IV compounds.

quite constant. Replacing the isopropyl group of the compounds represented by the left-hand structure of Scheme 6 (12^+ , 13^+ , and 30^+) by an aryl group to give the compounds represented by the second structure (32^+ – 34^+) causes a 27% drop in λ_v , while replacing the *tert*-butyl of these structures by a second phenyl group to give the third structure (35^+) causes a 26% drop in λ_v . The very large λ_v of hydrazines compared to other charge-bearing units is emphasized by the fact that removing the fourth alkyl substituent of the left-hand structure to give the trialkyldiazeniums represented by the right-hand structure causes a 57% drop in λ_v .

It is especially significant to compare these optically derived λ_v values with information from a completely separate source, intermolecular ET reactions involving the related monohydrazines **36**–**38** (Fig. 4). Marcus pointed out that intrinsic rate constants (those for zero driving force reactions) are the significant ones to consider for intermolecular ET reactions, and developed cross-rate theory to determine them.⁸³ Despite the fact that cross-rate theory was derived assuming that ET reactions are adiabatic, and it is now well known that they are not,¹⁶ cross-rate theory works so well when restricted to 0, +1 couples for which formal oxidation potentials can be measured accurately in acetonitrile that it can be used to reliably establish intrinsic rate constants by fitting experimental cross-rate constants and oxidation potential differences to Marcus cross-rate theory.⁸⁴ Although it is necessary to know the electronic coupling (V_{ab}) to determine the ET barrier and it is difficult to experimentally establish such numbers, the intrinsic rate constants can be turned into Eyring barriers ($\Delta G_{ii}^\ddagger(\text{fit})$ values) to allow their comparison. The absolute values of $\Delta G_{ii}^\ddagger(\text{fit})$ are not significant because no one thinks the Eyring pre-exponential factor

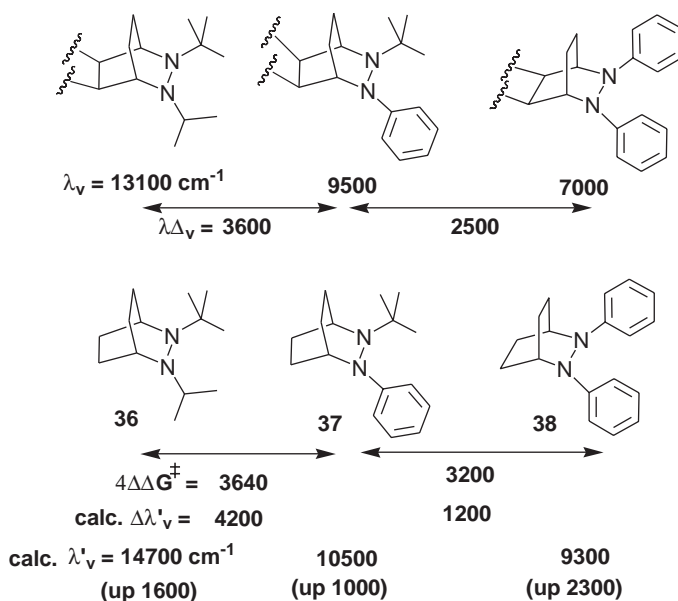


Fig. 4 Comparison of optically derived λ_v values with UB3LYP/6-31+ G^* -calculated λ_v values,^{24,82} and with experimental intermolecular intrinsic barriers for **36**^{0/+}–**38**^{0/+}.

is proper to use for ET reactions, but their relative values are significant linear measures of differences in intermolecular ET reactivity. The difference between the optically derived λ_v values for **M** = **36**– and **37**–centered *IV* compounds is within experimental error of what is obtained experimentally for four times the difference in $\Delta G_{\text{fit}}^{\ddagger}$ values (the factor of 4 is used because $\lambda/4$ appears in barriers). The $\Delta\Delta G^{\ddagger}$ value is 28% larger than the $\Delta\lambda_v$ value for the corresponding **37**, **38** comparison. The enthalpy contribution to intermolecular λ_v (which we call λ'_v) can be calculated.^{24,85} Unpublished results of such calculations at the B3LYP/6–31G* level are included in Fig. 4.⁸² The λ'_v values for the self-ET reactions (which include no electronic coupling) are larger than the experimental values for the *IV* compounds by 1000–2300 cm⁻¹. Because there is electronic coupling between the **M** units of the *IV* compounds, the calculated λ'_v values should be somewhat larger than the experimentally determined ones. It is not yet clear whether the scatter arises more from errors in the analysis of the experimental measurements or the calculated values. If the calculated λ'_v values are used in analysis of the intermolecular data, it results in the interpretation that the intermolecular V_{ab} increases as phenyls are substituted for alkyls in this series. This seems quite possible to us, but this question is too complex to deal with here.⁸⁶

We also note that the average λ'_v is 9700 ± 400 cm⁻¹ (only a $\pm 4\%$ range) when the five *IV* compounds that incorporate 2–*tert*-butyl-3–aryl-2,3–diazabicyclo[2.2.2] octane groups, as part of the bridge (**18**⁺, **20**⁺–**21**⁺, and **25**⁺–**26**⁺), are included as well as the saturated-bridged compounds (**32**⁺–**34**⁺). These λ_v values imply that it is rather misleading to restrict the definition of the “charge-bearing unit” **Hy** to the group shown as **15** for the aryl-bridged compounds; the aryl group must be at least partly included in **M**. This idea is also implied by the d_{ab} values discussed above, which are smaller than the distance between “the midpoints of the **M** groups” (however this rather fuzzy statement is defined). Nevertheless, the two-state model works as well for the π -bridged as for the σ -bridged compounds, so the spilling of charge onto the bridge, which always occurs for *IV* compounds, is handled by the model.

Turning our attention to the λ_s values obtained by the separation of λ_v from λ_s using optical spectroscopy, Fig. 5 shows a plot of the λ_s values of Table 7 versus the number of bonds between the N groups of phenyl, *tert*-butyl systems. These data indicate that a basic assumption of theories that we have seen used to calculate λ_s is incorrect. They assume that solvation of the cationic **M** group and the distance between them are all that needs to be considered. We suggest that these data demonstrate that solvation of the bridge is also important, because whether the bridge is saturated or not is clearly at least as important a factor for determining λ_s as distance, at least in the distance range examined.

7 Calculation of k_{opt} from optical data using adiabatic theory

The above discussion only considered room temperature optical spectra, but the rate data were usually taken at various temperatures. Varying the temperature changes \bar{v}_{max} , ε_{max} , and bandwidth (and hence quartic coefficient, Q value), as shown in

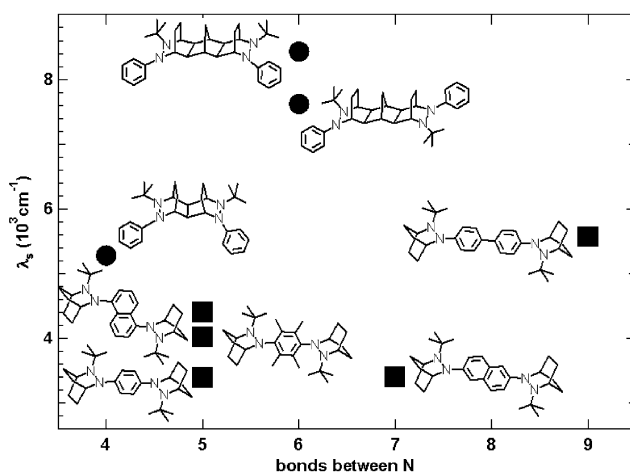


Fig. 5 Plot of optically derived λ_s in acetonitrile versus number of bonds between the hydrazines for phenyl, *tert*-butyl-substituted *IV* radical cations. The circles show saturated-bridged compounds, and the squares aromatic-bridged ones.

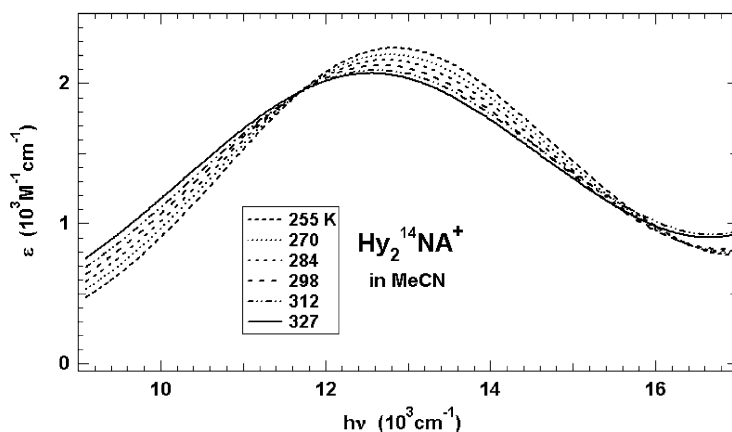


Fig. 6 Superimposed spectra of $\text{Hy}_2^{14}\text{NA}^+$ (24^+) as a function of temperature between 255 and 327 K in acetonitrile.

Fig. 6 for one example.⁴⁰ The band maximum $\bar{\nu}_{\text{max}}$ decreases within experimental error linearly in polar solvents, but noticeable curvature is observed in the ion-pairing solvent CH_2Cl_2 , as shown in **Fig. 7**. These band maxima are λ using MH theory with parabolic diabatic surfaces, and only slightly smaller than λ using quartic-adjusted diabatic surfaces that fit the observed bandwidth. **Table 8** shows the sensitivity of $\bar{\nu}_{\text{max}}$ to temperature.

Although all three components of Equation (5) are sensitive to temperature, the changes nearly cancel, and result in the electronic coupling V_{ab} calculated using Equation (4) with a constant d_{ab} being nearly constant. The largest change found

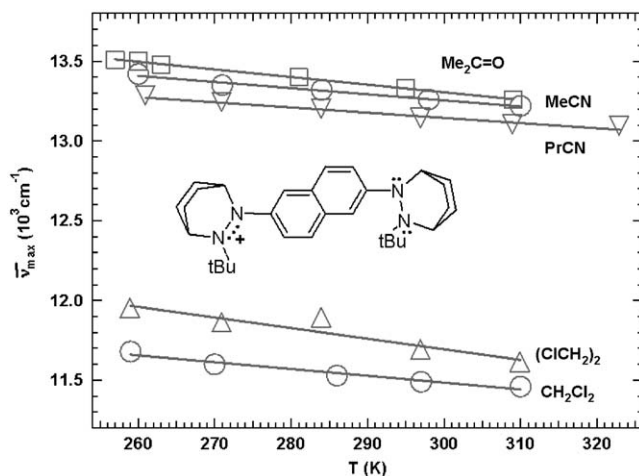


Fig. 7 Temperature dependence of $\bar{\nu}_{\max}$ for 26^+ $\text{Hy}_2^{26}\text{NA}^+$ in five solvents.

Table 8 T dependence of $\bar{\nu}_{\max}$ expressed as $E_{\text{op}} = A + BT$

| | Bridge ^a | Solvent | T range | A | B | Ref. |
|--------|----------------------|----------------------------|-----------|------------------|------------------|------|
| 19^+ | XY (5) | CH_3CN | 255–327 | $15,389 \pm 25$ | -3.56 ± 0.09 | 40 |
| 20^+ | DU (5) | CH_3CN | 255–326 | $15,236 \pm 35$ | -3.90 ± 0.12 | 40 |
| 21^+ | BI (9) | CH_3CN | 256–326 | $16,496 \pm 47$ | -4.27 ± 0.16 | 40 |
| 22^+ | FL (9) | CH_3CN | 255–298 | $14,506 \pm 118$ | -3.19 ± 0.43 | 40 |
| 24^+ | ^{14}NA (5) | CH_3CN | 255–327 | $13,939 \pm 24$ | -4.20 ± 0.08 | 40 |
| 26^+ | ^{26}NA (7) | CH_3CN | 260–310 | $14,429 \pm 59$ | -3.94 ± 0.21 | 42 |
| 26^+ | ^{26}NA (7) | PrCN | 261–323 | $14,123 \pm 85$ | -3.26 ± 0.29 | 42 |
| 26^+ | ^{26}NA (7) | CH_2Cl_2 | 259–324 | $12,284 \pm 301$ | -2.52 ± 1.03 | 42 |
| 26^+ | ^{26}NA (7) | $(\text{CH}_2\text{Cl})_2$ | 259–322 | $13,318 \pm 216$ | -5.38 ± 0.74 | 42 |

^aThe number in parentheses is the number of bonds between the N groups.

was a 6% decrease in V_{ab} as the temperature was raised 70° for Hy_2BI^+ (21^+), which is consistent with an increase in average twist about the central bond.

Changes in both μ_{12} and $\bar{\nu}_{\max}$ are observed as solvent is changed for both bis(hydrazines) and bis(diazeniums).⁷⁶ Nevertheless, V_{ab} was found to be rather constant to solvent changes as well, although a detectably smaller value was usually obtained in the least polar solvent studied, CH_2Cl_2 , for compounds that lack aryl groups. Including all 14 compounds, the total range in V_{ab} values including CH_2Cl_2 averages to 120 cm^{-1} and without CH_2Cl_2 60 cm^{-1} . We conclude that V_{ab} does not consistently depend upon solvent for these compounds, but might be different when significant ion pairing is present.

To compare with k_{ESR} , we calculate rate constants using the optically derived quartic-fitted parameters with the following rate expression:

$$k_{\text{opt}} = k_{\text{el}} \omega_{\text{p}} (\lambda_{\text{v}}/\lambda)^{1/2} \exp(-\Delta G^*/RT) \quad (17)$$

We estimate λ_v for use in calculating the $(\lambda_v/\lambda)^{1/2}$ term, which is rather close to one for hydrazines and therefore not very important, from the solvent effect studies.⁷⁶ The κ_{el} term is an attempt to extend the range for use of the adiabatic formula to somewhat less than completely adiabatic conditions. The value obtained for κ_{el} , evaluated as discussed by Sutin,⁸ is very close to 1 for our hydrazines, so they have large enough V_{ab} to undergo essentially adiabatic ET.

The energy of the barrier-crossing frequency, ω_v , is employed in the pre-exponential term.⁸ We used $\omega_v = 800 \text{ cm}^{-1}$ for bis(hydrazines), which is both close to the value estimated using semiempirical dynamics calculations on $\mathbf{11}^+$,³³ and obtained in as yet unpublished resonance Raman data for $\mathbf{20}^+$.⁸⁷ We used $\omega_v = 1100 \text{ cm}^{-1}$ for bis(diazonium) radical cations. This value is smaller than the 1403 cm^{-1} obtained from dynamics calculations on $\mathbf{sB4T}^+$ ($\mathbf{7}^+$)³³ but close to the 1053 cm^{-1} obtained from resonance Raman work in collaboration with Williams and Hupp.⁸⁸

Fig. 8 compares Eyring plots of the optical rate constants calculated using Equation (14) with the parameters listed in Table 8 with the ESR rate constants. The optical data are slightly different than those published earlier,⁴⁰ because they were fit using μ_{12} calculated using Equation (8) on refitted optical spectra, and different d_{12} values were used.⁸⁹ The ε_{max} value is not directly used in calculating the rate constant, because μ_{12} was obtained using Equation (8). Single^{34,66} and variable temperature results for several more compounds have been published,^{40,42} but the above examples suffice to show the remarkable agreement obtained between k_{opt} and k_{ESR} using the adiabatic rate equation, especially when the two measurements can be made in the same temperature region for non-ion-pairing solvents, which is not always the case. A vertical distance of 0.7 units on the Y-axis of Fig. 8 corresponds to a factor of two in the rate constant. The optical data produces larger $\ln(k/T)$ versus $1/T$ slopes than the ESR data, but it is not obvious that the ESR slopes are more reliable. The ESR data can only be taken over a narrow temperature range because the spectra stop changing significantly, and the fitting of the complex and

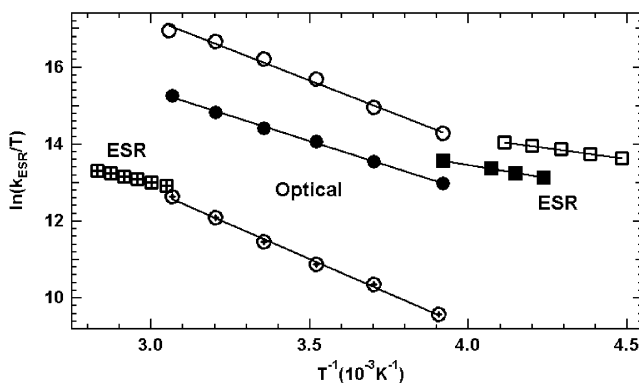


Fig. 8 Comparison of Eyring plots of k_{opt} (circles) calculated using Equation (14) with k_{ESR} (squares) for $\text{Hy}_2^{14}\text{NA}^+$ ($\mathbf{24}^+$, open symbols), Hy_2DU^+ ($\mathbf{20}^+$, filled symbols), and Hy_2BI^+ ($\mathbf{21}^+$, symbols with a cross).

Table 9 ET parameters used in calculating the rate constants plotted in Fig. 7

| Quantity | Hy ₂ ¹⁴ NA ⁺ | Hy ₂ DU ⁺ | Hy ₂ BI ⁺ |
|---|---|---------------------------------|---------------------------------|
| $\bar{\nu}_{\max}$ (cm ⁻¹) | 12,640 | 14,220 | 15,280 |
| ϵ_{\max} | 2120 | 970 | 2590 |
| Q | 0.008 | 0.19 | 0.02 |
| μ_{12} (D) | 3.05 | 2.196 | 3.18 |
| D_{12} (Å) | 4.61 | 5.70 | 8.41 |
| V_{ab} | 1510 | 1040 | 1080 |
| k_{opt} (10 ⁸ s ⁻¹) | 31.4 | 5.35 | 0.28 |

overlapping ESR spectra is far more difficult than determining the optical parameters of Table 9. As discussed in Section 4 (p. 200), the proper d_{12} to use is not obvious, and is the least well-known parameter, because it cannot be measured directly. It appears that Equation (14) agrees with k_{ESR} as well as d_{12} can be estimated, which was certainly not the result we had expected when we started this work.

The optical spectra of *anti* and *syn* 6-bond-bridged bis(diazenium) radical cations **14**⁺ were studied at 296 K in MeCN, PrCN, DMF, DMSO, and CH₂Cl₂ without finding significant differences between the diastereomers.^{37b} The ϵ_{\max} values ranged from 208 to 289 M⁻¹ cm⁻¹, and μ_{12} from 1.16 to 1.30 Debye, with the larger values in acetonitrile and methylene chloride. Their *IV* bands were unusually broad, $Q = 0.31$ – 0.40 in these solvents. The $k_{\text{opt}}/k_{\text{ESR}}$ values using $d_{12} = 5.62$ Å, which gave $d_{\text{ab}} = 5.64$ – 5.62 Å, V_{ab} values of 473–577 (highest in more polar solvents) and κ_{el} values of 0.86–0.78 were 3.3–4.7 in the solvents not expected to have strong ion-pairing effects, and 7.4–7.6 in CH₂Cl₂, presumably larger because ion pairing was not accounted for. The V_{ab} values obtained decrease nearly linearly with temperature, with temperature coefficients of about -0.3 cm⁻¹ K⁻¹ in acetonitrile and less in other solvents.^{37b} The **s14**⁺ optical spectrum was studied at variable temperature and gave activation parameters $\Delta H^{\ddagger} = 4.3 \pm 0.6$ kcal mol⁻¹, $\Delta S^{\ddagger} = -4.1 \pm 2.2$ for k_{opt} which are not statistically significantly different from the $\Delta H^{\ddagger} = 4.5 \pm 0.6$ kcal mol⁻¹, $\Delta S^{\ddagger} = -6.5 \pm 1.9$ found for k_{ESR} (Table 4). These lower V_{ab} systems have several problems, including small differences in first and second ionization potential, so there was a significant amount of neutral diradical present. This probably does not affect the ESR rate constant significantly, but may affect the optical studies more, since the triplet presumably absorbs in the *IV* band region, but is spin forbidden to undergo ET.

8 BJ treatment for ET within *IV* compounds

BJ theory replaces the classically derived energy surfaces and transition-state model of the MH treatment (Figs. 1 and 2) with a quantum-mechanical tunneling model. The BJ diabatic energy surfaces are shown in Fig. 9⁹⁰ Only the solvent is treated classically, and the *X*-axis now only represents solvent reorganization. Both energy

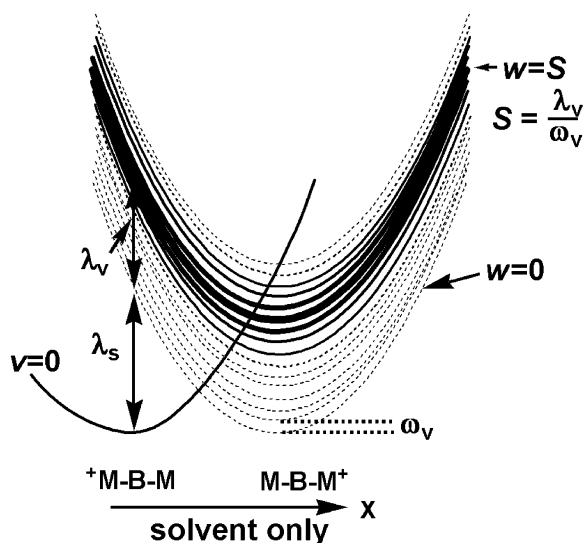


Fig. 9 Energy diagram for BJ treatment of an *IV* compound having $S = 11$.

wells contain a ladder of parabolas separated by ω_v , although for clarity, only the $v = 0$ parabola is shown on the left. The concept of a transition-state barrier is replaced by sums of tunneling factors, one for each starting material or product v or w well to each product or starting material w or v well. The sum of these tunneling factors constitutes the FCWD term in the BJ equation as shown below:

$$k_{\text{BJ}} = (2\pi/\nabla)|V_{\text{ab}}^2|(\text{FCWD}) \quad (18)$$

For the $\Delta G^\circ = 0$ case of a symmetrical *IV* compound, the starting material to product and product to starting material tunneling are equally effective. The value of S , the electron–vibrational coupling constant or Huang–Rhys factor, λ_v/ω_v , is obviously very important using BJ theory. As indicated in Fig. 8, which is drawn for an $S = 11$ case (about the size for H_2DU^+) and has the relative weighting of the tunneling factors indicated by the heaviness of the parabola line, the largest intensity occurs for $0, S$ transitions, and the intensities damp-off rapidly on both sides of S . The more familiar single sum (over v) “Golden Rule” FCWD that is used for large ΔG° reactions⁹¹ should be replaced by the double sum of the following equation:⁹²

$$\begin{aligned} \text{FCWD} &= [\sum_v \exp(-v\omega_v/k_B T)]^{-1} / (4\pi\lambda_s k_B T)^{-1/2} \\ &\sum_v \sum_w F(v, w) \exp(-v\omega_v/k_B T) \exp[-(\Delta G^\circ + \lambda_s + \{v - w\}\omega_v)^2 / 4\lambda_s k_B T] \\ F(v, w) &= \exp(-S)v!w! [\sum_r \{(-1)^{v+w-r} S^{(v+w-2r)/2}\} / \{r!(v-r)!(w-r)!\}]^2 \end{aligned} \quad (19)$$

$F(v, w)$ in Equation (19) is the Franck–Condon factor for v – w coupling, and the sum is from $r = 0$ to the minimum of v and w . As shown in Fig. 10,⁹³ which gives plots of V_{ab} versus ω_v values that fit $k_{\text{ET}}(25^\circ\text{C}) = 1.32 \times 10^8 \text{ s}^{-1}$ for a $\Delta G^\circ = 0$ ET when $\lambda_v = 13,150 \text{ cm}^{-1}$, $\lambda_s = 3150 \text{ cm}^{-1}$ (values for $\mathbf{11}^+$) using adiabatic rate theory

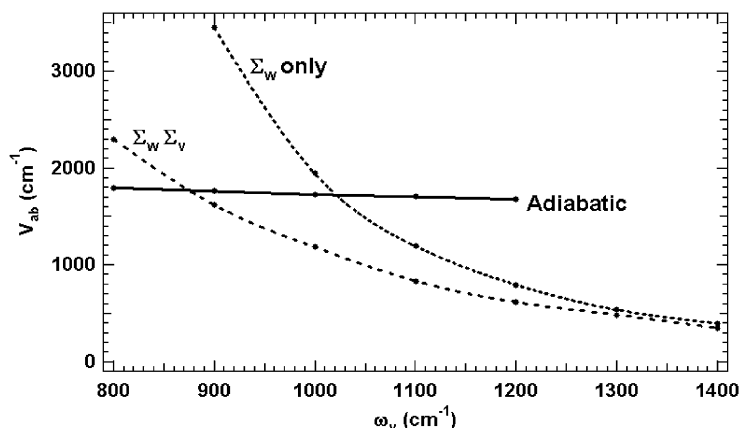


Fig. 10 Fit to $k_{\text{ET}} = 1.32 \times 10^8 \text{ s}^{-1}$, $\lambda_v = 13,150 \text{ cm}^{-1}$, $\lambda_s = 3150 \text{ cm}^{-1}$, $\Delta G^\circ = 0$ using the adiabatic equation (17), and with Equation (19) and the single sum BJ equation.

(Equation 14) and BJ theory with the “Golden rule” single sum FCWD and the with the double sum FCWD of Equation (19). Fig. 10 shows how small the effect of using ω_v as a simple multiplier in Equation (17) is compared to using it in the exponential terms, as in Equation (19). It will also be noted that for small ω_v values the BJ theory predicted V_{ab} exceeds that produced by the adiabatic limit using the parameters quoted.

Using BJ theory, there is no transition state. The English words used in talking about $\lambda = \lambda_s + \lambda_v$ are the same as for MH theory, although now λ is always somewhat larger than $\bar{\nu}_{\text{max}}$ for a symmetrical IV compound, instead of being equal to it. The V_{ab} is the same in MH and BJ theory. Use of single “averaged” ω_v despite the fact that many modes are involved, each of which contributes an increment to λ_v has been justified.¹⁶ The averaging includes the square of the energy times its fractional contribution to λ_v^8 :

$$\langle \omega_v \rangle = \left(\sum_q [\omega_v(q)]^2 [\lambda_v(q)/\lambda_v] v \right)^{1/2} \quad (20)$$

We do not doubt that ET in these compounds is proceeding by tunneling, as Bixon and Jortner discuss.¹⁶ We believe that this is demonstrated for the Hy_2Ar^+ compounds by the substantial sensitivity of electronic coupling to position on the ET coordinate. Calculations at both semiempirical⁵⁷ and ab initio levels⁵⁸ clearly show that the $\text{C}_{\text{Ar}}\text{-N}$ twist angle ϕ is significantly smaller at the transition state than at the energy minimum. If the compounds went to the ET transition state, they would have far smaller barriers than is experimentally observed, because V_{ab} is expected to be roughly proportional to $\cos \phi$, and is observed to be so from our measurements on the series $\mathbf{18}^+ \text{-} \mathbf{20}^+$. We conclude that the twist angle when the electron is transferred is instead what it is at the energy minimum, which is where it is measured using MH theory. Confusingly, however, there is clearly something wrong with Equation (18), which does not predict the rate constants properly at all,

as we have pointed out for several systems.^{36–38} For example, Hy_2DU^+ , which has k_{ESR} values that are fit rather well by Equation (17) (Fig. 8), gives $k_{\text{BJ}}/k_{\text{opt}}$ ratios that drop from 40 at 255 K to 12 at 326 K when the optical spectra are analyzed using $\omega_{\text{v}} = 800$, $\lambda_{\text{v}} = 8290$, $\lambda_{\text{s}} = 6740 \text{ cm}^{-1}$. We are now convinced that changes in the λ_{v} , λ_{s} partitioning are not the problem. Our results therefore show that MH theory, which assumes that ET reactions go through a transition state which they rather clearly do not, as well as that V_{ab} is constant on the ET coordinate, which is not true for these compounds, provides much better estimates of the ET barriers than does estimation using the single-frequency BJ theory. We find this both surprising and disturbing. We have suggested that one problem is that BJ theory assumes that the surfaces are harmonic past S , which is unlikely to be true for compounds with large S , and noted that *IV* bis(diazoniums) are better fit by BJ theory than bis(hydrazines).³⁷ There may, however, be another explanation for the problems BJ theory has with fitting our data. Zhu and Nakamura point out that they actually have solved the two-state problems that were posed by Landau, Zerner, and Stückelberg in 1932 for electronic couplings in the chemically significant range, and that the solutions to two-state theory that have been used in previous theories are significantly in error in the chemically significant parameter region.⁹⁴ Zhu–Nakamura theory is mathematically complex and does not lead to compact equations; I certainly do not understand it. Zhao and Nakamura have submitted an article that I think is important,⁹⁵ which applies Zhu–Nakamura theory to ET, fitting our experimental ESR data on 2,7–dinitronaphthalene radical anion, obtaining quite different results from BJ theory.⁹⁶

9 Effects of low-bridge-oxidized excitation energies

Not all ET systems should be treated by the two-state model. In collaboration with Jeff Zink (University of California at Los Angeles) we have recently realized that Class III *IV* compounds should never be treated with the two-state model, because the simplest model that can give valid electronic couplings has four states and two different couplings.^{97–99} When the two-state model works for Class II compounds, the bridge provides electronic coupling between the \mathbf{M} groups (V_{ab}), and the orbital energies of the bridge do not need to be explicitly considered. This will only occur when the $(\mathbf{M}-\mathbf{B}^+-\mathbf{M})^*$ excited state is high enough in energy. As the $(\mathbf{M}-\mathbf{B}^+-\mathbf{M})^*$ energy decreases relative to λ , the two-state model will become less satisfactory, and eventually $\mathbf{M}-\mathbf{B}^+-\mathbf{M}$ will appear as a minimum on the ground-state energy surface, and the system becomes what is now called an incoherent electron-hopping one. Electron hopping is unquestionably the way that really long-distance ET is achieved in nature, and is currently a topic of great interest.¹⁰⁰ Although standard MH theory should work just fine to calculate rate constants if the ΔG° for the $\mathbf{M}^+-\mathbf{B}-\mathbf{M} \rightarrow \mathbf{M}-\mathbf{B}^+-\mathbf{M}$ step and the other ET parameters are known, there is basically no way to determine them in real systems. If the rate constant for an electron-hopping system is analyzed as if the electrons were jumping all the way from one \mathbf{M} to the other, especially using an exponential drop-off of V_{ab} with distance model, one obtains

enormous overestimations of electronic couplings, which has led to considerable discussion in the literature.

One does not have to make large structural changes for the two-state model to fail for Hy_2Ar^+ examples. Even though it works just fine for quantitatively predicting rate constants in the benzene, biphenyl, and naphthalene-bridged systems discussed in Section 3, there are already problems with $\text{Hy}_2^{9,10}\text{AN}^+$ (28^+) (Scheme 3). Fusing a second benzene ring onto the $\text{Hy}_2^{14}\text{NA}^+$ (24^+) introduces more twist, which will decrease V_{ab} , and one would therefore expect $\text{Hy}_2^{9,10}\text{AN}^+$ to have a smaller k_{ESR} value than $\text{Hy}_2^{14}\text{NA}^+$. This is not the case. Instead the $\text{Hy}_2^{9,10}\text{AN}^+$ k_{ESR} is comparable to that for Hy_2PH^+ , too fast to measure accurately by ESR, but estimated to be on the order of $150 \times$ larger than expected.⁴³ Its optical spectrum immediately shows what is wrong. For this compound, the IV band (which comes at about $14,000 \text{ cm}^{-1}$ for these 5-bond-bridged systems) is not the lowest-energy absorption. Instead its lowest-energy band is at $\bar{\nu}_{\text{max}} = 9000 \text{ cm}^{-1}$, $\epsilon_{\text{max}} = 1400$, $\Delta\bar{\nu}_{1/2} = 4300 \text{ cm}^{-1}$ (estimated from the low-energy side only because of overlap with other absorptions). We attributed this band to “bridge oxidation” ($\text{M}^+-\text{B}-\text{M} \rightarrow \text{M}-\text{B}^+-\text{M}$) and gave a simple two-dimensional three-state model that predicts that even though the vertical energy gap to the bridge oxidation state lies this far below the superexchange λ , $\text{M}-\text{B}^+-\text{M}$ is not predicted to be a minimum on the ground-state energy surface. The optical studies on the naphthalene-bridged systems indicate that for these compounds, where the bridge oxidation band lies above the superexchange λ , the same three-state model does not predict significantly different k_{ET} values from the two-state model, and experimentally, the two-state k_{opt} values are in agreement with k_{ESR} .⁴² A $\Delta G = 0$ electron-hopping IV compound has not yet been prepared.

Acknowledgements

I thank the many fine students and colleagues who carried out the experiments discussed here, and the National Science Foundation for its continued support of our program, currently under grant CHE-024019. I thank Asgeir Konradsson and Mike Weaver for valuable comments on the manuscript.

References

1. Robin, M.B. and Day, P. (1967). *Adv. Inorg. Radiochem.* **10**, 247–422
2. Allen, G.C. and Hush, N.S. (1967). *Prog. Inorg. Chem.* **8**, 357–390
3. Creutz, C. and Taube, H. (1969). *J. Am. Chem. Soc.* **91**, 3988–3989
4. Demadis, K.D., Hartshorn, C.M. and Meyer, T.J. (2001). *Chem. Rev.* **101**, 2655–2685
5. Cowan, D.O., LeVanda, C., Park, J. and Kaufman, F. (1973). *Account. Chem. Res.* **6**, 1–7
6. Hush, N.S. (1967). *Prog. Inorg. Chem.* **8**, 391–444
7. Marcus, R.A. and Sutin, N. (1985). *Biochim. Biophys. Acta* **811**, 265–322
8. Sutin, N. (1983). *Prog. Inorg. Chem.* **30**, 441–499
9. Creutz, C., Newton, M.D. and Sutin, N. (1994). *J. Photochem. Photobiol. A* **82**, 47–59
10. Kosloff, R. and Ratner, M.A. (1990). *Israel J. Chem.* **30**, 45–58

11. Mulliken, R.S. (1952). *J. Am. Chem. Soc.* **74**, 811–824
12. Brunschwig, B.S., Creutz, C. and Sutin, N. (2002). Optical transitions of symmetrical mixed-valence systems in the Class II–III transition regime. *Chem. Soc. Rev.* **31**, 168–184
13. Nelsen, S.F. (2000). *Chem. Eur., J.* **6**, 581–588
14. The constant term is $[(3000 \log(10)hc/8\pi^3N_A)/e]$, which using newer values for the constants is 0.01995. Hush also used an α multiplier for d_{ab} , but we have seen no one use a value other than $\alpha = 1$
15. Hush, N.S. (1985). *Coordin. Chem. Rev.* **64**, 135–157
16. Bixon, M. and Jortner, J. (1999). *Adv. Chem. Phys.* **106**, 35–202
17. Elliott, C.M., Derr, D.L., Matyushov, D.V. and Newton, M.D. (1998). *J. Am. Chem. Soc.* **120**, 11714–11726
18. We show reported errors in the last figure given in this chapter in parentheses: $0.24(1) = 0.24 \pm 0.01$
19. Nelsen, S.F. (1992). In *Acyclic Organonitrogen Stereodynamics*, Lambert, J.B. and Takeuchi, Y. (eds), Chapter 3, pp. 89–121. VCH, New York
20. Nelsen, S.F., Blackstock, S.C. and Haller, K.J. (1986). *Tetrahedron* **42**, 6101–6109
21. Nelsen, S.F. (1992). In *Acyclic Organonitrogen Stereodynamics*, Lambert, J.B. and Takeuchi, Y. (eds), Chapter 7, pp. 245–262. VCH, New York
22. Nelsen, S.F. and Blackstock, S.C. (1985). *J. Am. Chem. Soc.* **107**, 7189–7190
23. Nelsen, S.F., Frigo, T.B., Kim, Y., Thompson-Colón, J.A. and Blackstock, S.C. (1986). *J. Am. Chem. Soc.* **108**, 7926–7934
24. Nelsen, S.F., Blackstock, S.C. and Kim, Y. (1987). *J. Am. Chem. Soc.* **109**, 677–682
25. Nelsen, S.F., Kim, Y. and Blackstock, S.C. (1989). *J. Am. Chem. Soc.* **111**, 2045–2051
26. Nelsen, S.F. and Wang, Y. (1994). *J. Org. Chem.* **59**, 1655–1662
27. (a) Shen, K.W. (1971). *J. Chem. Soc. Chem. Commun.* 391–392; (b) Shen, K.W. (1971). *J. Am. Chem. Soc.* **93**, 3064–3066
28. Nelsen, S.F., Wolff, J.J., Chang, H. and Powell, D.R. (1991). *J. Am. Chem. Soc.* **113**, 7882–7886
29. Nelsen, S.F., Chang, H., Wolff, J.J. and Adamus, J. (1993). *J. Am. Chem. Soc.* **115**, 12276–12289
30. Nelsen, S.F., Blackstock, S.C. and Frigo, T.B. (1986). *Tetrahedron* **42**, 1769–1777
31. Nelsen, S.F., Wang, Y., Hiyashi, R.K., Powell, D.R. and Neugebauer, F.A. (1995). *J. Org. Chem.* **60**, 2981–2989
32. Nelsen, S.F., Adamus, J. and Wolff, J.J. (1994). *J. Am. Chem. Soc.* **116**, 1589–1590
33. Nelsen, S.F. (1996). *J. Am. Chem. Soc.* **118**, 2047–2058
34. (a) Previously unpublished calculations; (b) B3LYP/6-31G* calculations do not describe IV compounds properly (see Ref. [58]): they get **11-in⁺.in** to be the most stable conformation, but only a 0.005 Å *NN* distance difference between its two hydrazine units and a long axis dipole moment of only 0.6 Debye, both of which we believe are clearly incorrect
35. Nelsen, S.F., Chen, L.-J., Powell, D.R. and Neugebauer, F.A. (1995). *J. Am. Chem. Soc.* **117**, 11434–11440
36. Nelsen, S.F., Ramm, M.T., Wolff, J.J. and Powell, D.R. (1997). *J. Am. Chem. Soc.* **119**, 6863–6872
37. (a) Nelsen, S.F., Trieber, D.W.II, Wolff, J.J., Powell, D.R. and Rogers-Crowley, S. (1997). *J. Am. Chem. Soc.* **119**, 6873–6882; (b) Trieber, D.W. (2000). Ph.D. Thesis, University of Wisconsin, Madison, WI
38. Nelsen, S.F., Ismagilov, R.F. and Powell, D.R. (1996). *J. Am. Chem. Soc.* **118**, 6313–6314
39. Nelsen, S.F., Ismagilov, R.F. and Powell, D.R. (1997). *J. Am. Chem. Soc.* **119**, 10213–10222
40. Nelsen, S.F., Ismagilov, R.F., Gentile, K.E. and Powell, D.R. (1999). *J. Am. Chem. Soc.* **121**, 7108–7114

41. Nelsen, S.F. and Ismagilov, R.F. (1999). *J. Phys. Chem. A* **103**, 5373–5378
42. Nelsen, S.F., Konradsson, A.E. and Teki, Y. (2006). Charge-localized naphthalene-bridged bis-hydrazine radical cations. *J. Am. Chem. Soc.* **128**, 2902–2910
43. Nelsen, S.F., Ismagilov, R.F. and Powell, D.R. (1998). *J. Am. Chem. Soc.* **120**, 1924–1925
44. Ismagilov, R.F. (1998). Ph.D. Thesis, University of Wisconsin, Madison, WI
45. Hush originally⁶ used a more complex criterion for bandwidth, $I_v \bar{v}_{\max}/I_{\max} \bar{v}_{\max} = 1/2$, which reflects the fact that in theory, bands are only Gaussian when ϵ/\bar{v} is plotted versus \bar{v} , but experimentalists never took to implementing this, and he later switched to the form usually quoted. The correction is rather minor, and the experimental bands are not exactly Gaussian plotted either way
46. Nelsen, S.F., Ismagilov, R.F. and Trieber II, D.A. (1997). *Science* **278**, 846–849
47. Gould, I.R., Noukakis, D., Gomez-Jahn, L., Youg, R.H., Goodman, J.L. and Farid, S. (1993). *Chem. Phys.* **176**, 439–456
48. Liptay, W. (1969). *Angew Chem. Int. Edit. Engl.* **8**, 177–188
49. Gould, I.R., Young, R.H., Mueller, J.L. and Farid, S. (1994). *J. Am. Chem. Soc.* **116**, 8176–8187
50. Chako, N.Q. (1934). *J. Chem. Phys.* **2**, 644–653
51. Calvert, J.G. and Pitts, J.N.Jr. (1966). *Molecular Photochemistry*. New York, Wiley (p.172)
52. Rubinowicz, A. (1948–1949). *Rep. Prog. Phys.* **12**, 233
53. Cave, R.J. and Newton, M.D. (1996). *Chem. Phys. Lett.* **249**, 15–19
54. Cave, R.J. and Newton, M.D. (1997). *J. Chem. Phys.* **106**, 9213–9226
55. Nelsen, S.F. and Newton, M.D. (2000). *J. Phys. Chem. A* **104**, 10023–10031
56. Johnson, R.C. and Hupp, J.T. (2001). *J. Am. Chem. Soc.* **123**, 2053–2057
57. Blomgren, F. and Nelsen, S.F. (2001). *J. Org. Chem.* **66**, 6551–6559
58. Blomgren, F., Larsson, S. and Nelsen, S.F. (2001). *J. Comput. Chem.* **22**, 655–664
59. Oh, D.H. and Boxer, S.G. (1990). *J. Am. Chem. Soc.* **112**, 8161
60. Oh, D.H., Sano, N. and Boxer, S.G. (1991). *J. Am. Chem. Soc.* **113**, 6880
61. Bublitz, G.U. and Boxer, S.G. (1997). *Annu. Rev. Phys. Chem.* **48**, 213–242
62. Bublitz, G.U., Ortiz, R., Runser, C., Fort, A., Marzoukas, M., Marder, S.R. and Boxer, S.G. (1997). *J. Am. Chem. Soc.* **119**, 2311–2312
63. Bublitz, G.U., Laidlaw, W.M., Denning, R.G. and Boxer, S.G. (1998). *J. Am. Chem. Soc.* **120**, 6068
64. Karki, L., Lu, H.P. and Hupp, J.T. (1996). *J. Phys. Chem.* **100**, 15637
65. Karki, L., Williams, R.D., Hupp, J.T., Allan, C.B. and Spreer, L.O. (1998). *Inorg. Chem.* **37**, 2837–2840
66. Vance, F.W. and Hupp, J.T. (1999). *J. Am. Chem. Soc.* **121**, 4047–4053
67. Walters, K.A., Gaal, D.A. and Hupp, J.T. (2002). *J. Phys. Chem. B* **106**, 5139–5142
68. Walters, K.A., Kim, Y.-J. and Hupp, J.T. (2002). *Inorg. Chem.* **41**, 2009–2019
69. Shin, Brunschwig, B.S., Creutz, C. and Sutin, N. (1995). *J. Am. Chem. Soc.* **117**, 8668–8669
70. Shin, Y.K., Brunschwig, B.S., Creutz, C. and Sutin, N. (1996). *J. Phys. Chem.* **10**, 8157–8169
71. Hirota, N. and Weissman, S.I. (1964). *J. Am. Chem. Soc.* **86**, 2538
72. Dvolaitzky, M., Chiarelli, R. and Rassat, A. (1992). *Angew. Chem. Int. Edit. Engl.* **31**, 180
73. Piotrowiak, P. and Miller, J.R. (1993). *J. Phys. Chem.* **97**, 13052–13060
74. Kuznetsov, A.M., Phelps, D.K. and Weaver, M.J. (1990). *Int. J. Chem. Kinet.* **22**, 815
75. Nelsen, S.F., Konradsson, A.E., Clennan, E.L. and Singleton, J. (2004). *Org. Lett.* **6**, 285–287
76. Nelsen, S.F., Trieber, D.A.II, Ismagilov, R.F. and Teki, Y. (2001). *J. Am. Chem. Soc.* **123**, 5684–5694

77. Nelsen, S.F., Konradsson, A.E., Ismagilov, R.F. and Guzei, I.A. (2005). *Crystal Growth Des.* **5**, 2344–2347
78. Chen, P. and Meyer, T.J. (1998). *Chem. Rev.* **98**, 1439–1477
79. (a) Pekar used it as a principal factor in phonon theory, published in textbook form by 1951; (b) Pekar, S.I. (1954). *Untersuchen über die Elektronentheorie der Kristalle*. Akademie-Verlag, Berlin (Russian edition, 1951)
80. (a) *Ber. Bunsenges. Phys. Chem.* **88**(1984), 325–334; (b) Grampp, G. and Jaenicke, W. (1984). *Ber. Bunsenges. Phys. Chem.* **88**, 335–340
81. (a) Gutmann, V. (1976). *Coordin. Chem. Rev.* **18**, 225; (b) Gutmann, V. (1980). *The Donor–Acceptor Approach to Molecular Interactions*. New York, Plenum
82. Weaver, M.N. (2006). Ph.D. Thesis, University of Wisconsin, Madison, WI
83. Marcus, R.A. (1956). *J. Chem. Phys.* **24**, 966–978
84. Nelsen, S.F. and Pladziewicz, J.R. (2002). *Account. Chem. Res.* **35**, 247–254 and references therein
85. It can also be calculated for *IV* compounds, and we have found semiempirical AM1 calculations of λ'_v to be useful. There is, however, a significant problem with trying to improve these calculations to include large basis sets. UHF calculations get enormous spin contamination and make bad errors in geometry that make them less accurate than AM1 calculations for obtaining λ'_v of hydrazines (strange as this statement may sound, it is true). B3LYP calculations are excellent for monohydrazines, but fail for *IV* compounds because they improperly delocalize charge too much, for example, getting the localized compounds of Scheme 4 to be delocalized.⁵⁸ We therefore do not discuss such calculations here, except to mention that AM1 calculations show that λ'_v for *IV* compounds are indeed increasingly smaller than for the isolated *M* groups as calculated electronic coupling increases⁵⁷
86. Nelsen, S.F., Weaver, M.N., Pladziewicz, J.R., Ausman, L., Jentsch, T.L. and O'Konneck, J.J. *J. Phys. Chem. A* (in press)
87. Resonance Raman work carried out by Jenny Lockhard and Jeffrey I. Zink at University of California at Los Angeles, to be published
88. Williams, R.D., Hupp, J.T., Ramm, M.T. and Nelsen, S.F. (1999). *J. Phys. Chem. A* **103**, 11172–11180
89. Previously unpublished calculations by Asgeir E. Konradsson
90. We thank Ralph Young of Kodak for detailed discussion of this drawing
91. Liang, N., Miller, J.R. and Closs, G.L. (1990). *J. Am. Chem. Soc.* **112**, 5353–5354
92. (a) Cortes, J., Heitele, H. and Jortner, J. (1994). *J. Phys. Chem.* **98**, 2527; (b) We thank Prof. Jortner for explaining the proper use of this equation
93. Redrawn from Ref. 33, with corrected values (Ref. 36, Footnote 20)
94. (a) Zhu, C. and Nakamura, H. (1994). *J. Chem. Phys.* **101**, 10630–10647; (b) Zhu, C. and Nakamura, H. (1995). *J. Chem. Phys.* **102**, 7448–7461; (c) Zhu, C., Teranishi, Y. and Nakamura, H. (2001). *Adv. Chem. Phys.* **117**, 127–233
95. Zhao, Y. and Nakamura, H. *Theor. Comput. Chem* (in press)
96. Nelsen, S.F., Weaver, M.N., Konradsson, A.E., Telo, J.P. and Clark, T. (2004). *J. Am. Chem. Soc.* **126**, 15431–15438
97. Nelsen, S.F., Weaver, M.N., Telo, J.P. and Zink, J.I. (2005). *J. Am. Chem. Soc.* **127**, 11611–11622
98. Nelsen, S.F., Luo, Y., Weaver, M.N., Lockard, J.V. and Zink, J.I. (2006). *J. Org. Chem.* **71**, 4286–4295
99. Nelsen, S.F., Weaver, M.N., Luo, Y., Lockard, J.V. and Zink, J.I. (2006). *Chem. Phys.* **324**, 195–201
100. Gray, H.B. and Winkler, J.R. (2005). *Proc. Nat. Acad. Sci. USA* **102**, 3534–3539